3. Results and Discussion

3.1. Characterization of the raw clay

3.1.1. X-Ray diffraction analysis (XRD) of the raw clay

These results include the study of XRD of the bulk clay samples as well as the treated samples. Treated samples include oriented, glycolated and heated samples.

Fig (6) shows XRD of the powder bulk clay and comparing with the ASTM cards for non-clay minerals. It is evident that quartz (SiO_2) is the main non clay mineral in addition to lesser amounts of feldspar (alkali alumino-silicates) and goethite ($Fe_2O_3 .H_2O$) .

Fig (7) shows the X-ray diffraction patterns of the bulk and clay fraction (oriented mounts), the three essential clay minerals are montmorillonite that is characterized by its strongest d-line (d=14.15 A^0,4.50 A^0 and 3.02 A^0 and others); Kaolinite is characterized by its strongest d-line (d=7.10 A^0 , 3.56 A^0 and 4.41 A^0 and others) and Illite is characterized by its strongest d-line (d=10.00 A^0 ,4.48 A^0 and 3.33 A^0 and others). On the other hand, quartz is characterized by its strongest d-lines (d=3.34 A^0 and 4.26 A^0 and others) [4,39] .

Table (5) shows clay minerals content as semi quantitatively determined from XRD pattern of the oriented clay fraction Fig (7).

Table (5): Wt % of clay minerals.

Clay Minerals	Montmorillonite	Kaolinite	Illite
Wt %	39.1	35.3	25.6

The results of Fig (7) and Table (5) show that the used clay deposit is composed of montmorillonite, kaolinite and illite clay minerals in a decreasing order of abundance. Montmorillonite is characterized in Fig (7) by a basal reflection peak at 15.0 A^0 upon treated with ethylene glycol this peak is expanded to 17.0 A^0 and completely eliminated by heating up to 550 ^{0}C conferring the presence of montmorillonite . The basal reflection of kaolinite which exist at 7.2 A^0 is not affected by ethylene glycol and eliminated on heating to 550 ^{0}C. On the other hand the basal reflection of illite 10.0 A^0 is not affected neither by ethylene glycol nor by heating [37].

3.1.2. Differential thermal analysis (DTA)

Thermal behavior of the batch has been revealed from the differential thermal analyses data (DTA) as follows:

With heating, the batch undergoes different physical, chemical and mineralogical reactions. Such reactions and the temperatures corresponding to their maximum intensity can be summarized as follows:-

a- Evolution of residual hygroscopic and interlayer water of montmorillonite and illite clay minerals (130 ^{o}C), endothermic peak.
b- Dehydration of goethite (274 ^{o}C).
c- Dehydroxylation of lattice water of montmorillonite, illite and kaolinite clay minerals (504 ^{o}C).
d- Quartz transformation $\alpha \rightarrow \beta$ form (573 ^{o}C).
e- Between 850 and 900 ^{o}C an endothermic peak corresponding to dissociation of dolomite and calcium carbonate.

During cooling, the most important change is the $\beta \rightarrow \alpha$ quartz transformation (573 ^{o}C) which is exothermic in nature [47].

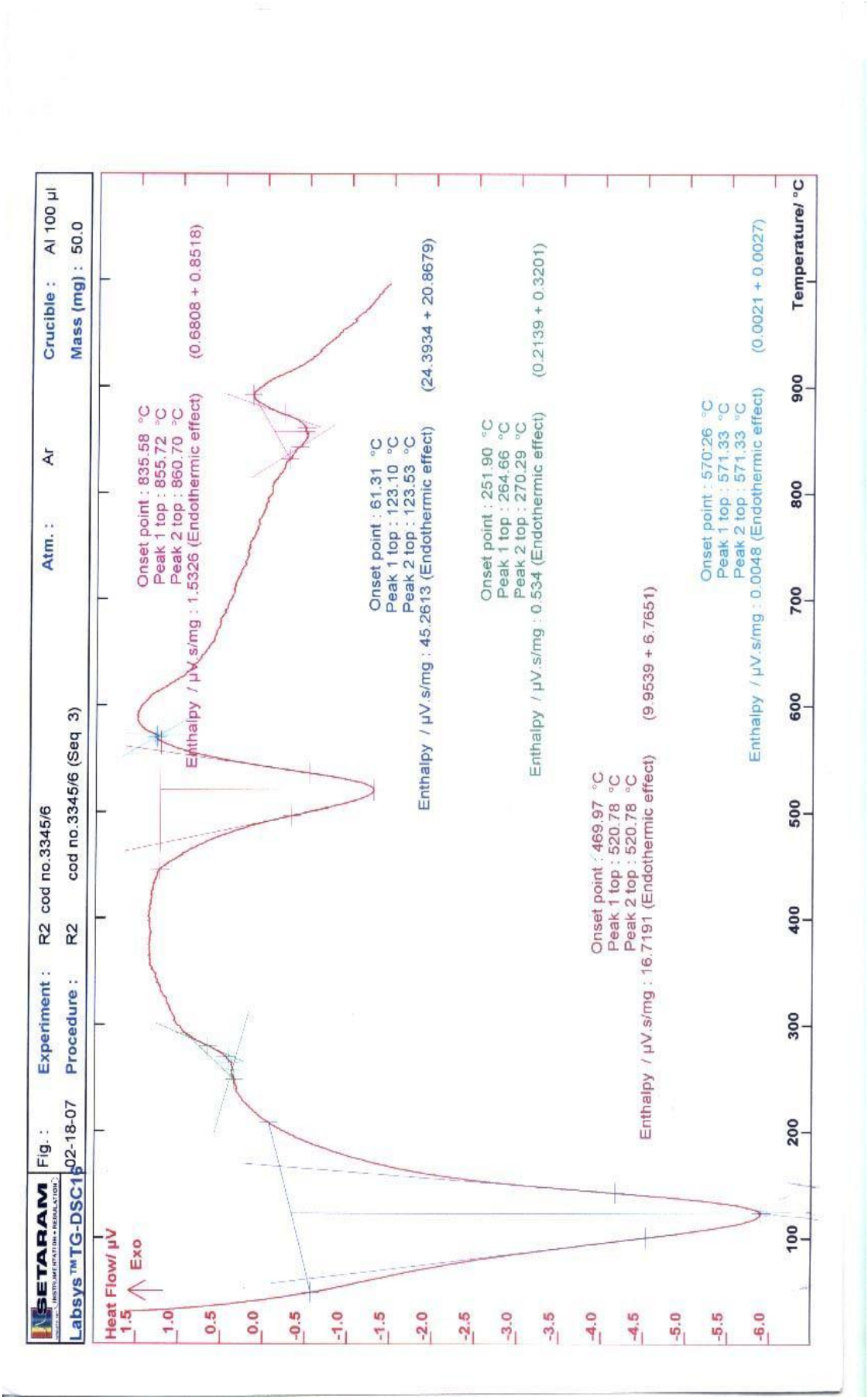

Fig (8): The DTA of the clay sample

3.1.3. Particle size analysis of the clay sample

Table (6) shows particle size distribution of the raw clay sample. It consists of 9.46 % sand, 51.05 % silt and 39.49 clay. The results were also plotted on folks clay-silt-sand ternary diagram [5], as shown in Fig (9). It is evident that the raw clay sample lies in the muddy region in the diagram due to the predominance of its fine fraction content (90.54%) with low amount of sand particles (9.46%). It doesn't belong to the balanced composition of the sandy mud required for the clay bricks manufacture. That indicate that the studied raw clay needs addition of relatively coarse fraction as opening agent to be adequate for clay bricks manufacture .

Table (6): Particle size distribution of the clay sample.

Particles	**Gravel**	**Sand**	**Silt**			**Clay**
Size (mm)	**> 2.0**	**> 63µm**	**63-16 µm**	**16-8µm**	**8-2µm**	**< 2 µm**
(%)	**-**	**9.46**	**11.21**	**19.36**	**20.48**	**39.49**

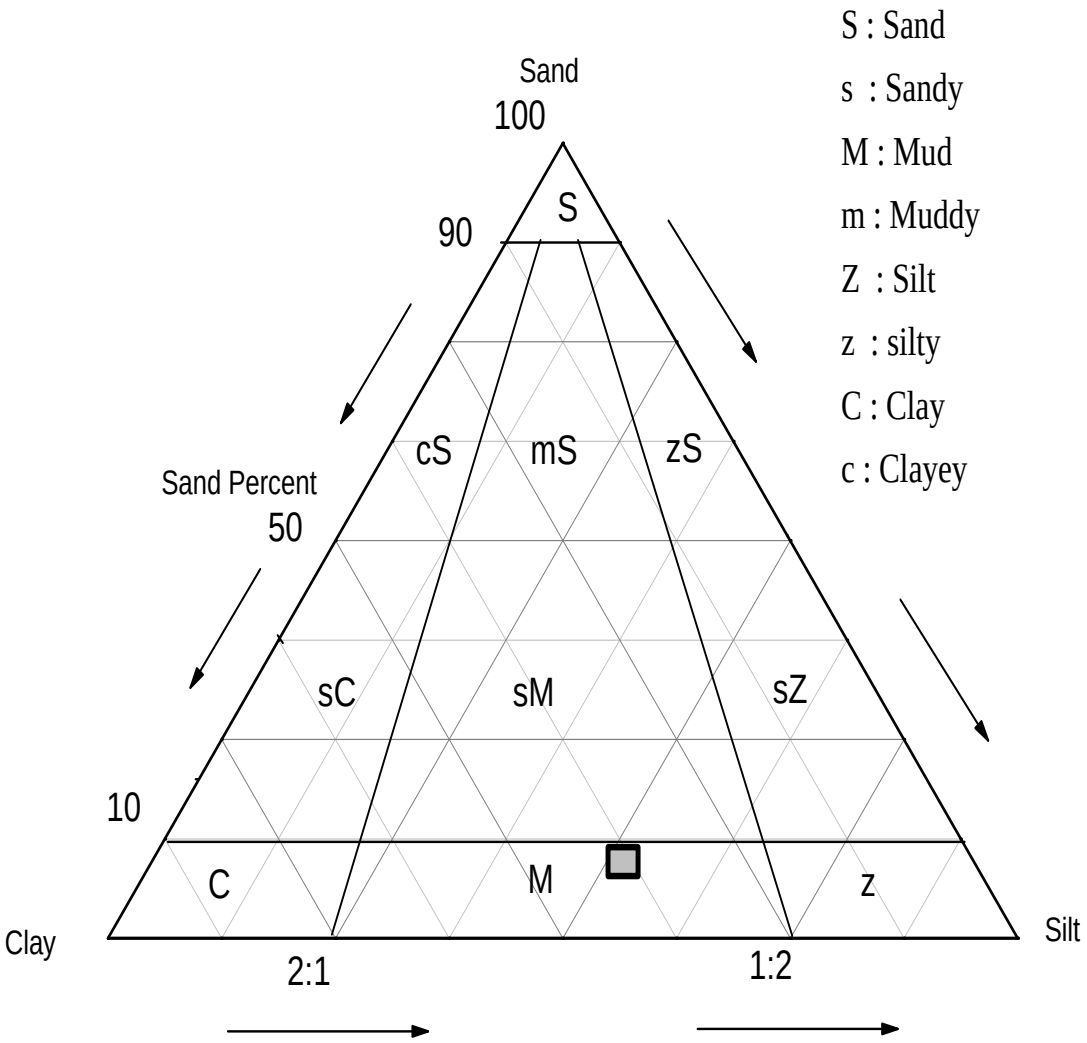

Fig (9): The Clay-Silt-Sand Ternary Diagram.

3.1.4. Chemical Composition (XRF) for the clay sample.

Table (7) illustrates that the major constituents in the raw clay are SiO_2, Al_2O_3 and Fe_2O_3 in a descending order. The high SiO_2 and low Al_2O_3 content are mainly due to the predominance of montmorillonite clay mineral as well as the presence of considerable amounts of quartz (SiO_2) and feldspar (alkali alumino-silicates) as non clay minerals. The high Fe_2O_3content (10.86%) is mainly attributed to the presence of appreciable amount of the hydrated iron oxide mineral goethite (Fe_2O_3 $3H_2O$), it gives the bricks the red colour.

In addition to Fe_2O_3 , smaller amounts of TiO_2,Cao,MgO,Na_2O and K_2O are detected as impurity oxides. These oxides may exist as isomorphous substitutions within the lattice of clay minerals and / or as non –clay minerals.

From the chemical analysis data, the studied clay sample can be considered as low grade clay referring to its low content of Al_2O_3 and its considerable content of the impurity oxides: Fe_2O_3, Na_2O, K_2O …. etc which act as fluxing agents to the refractory oxides , causing the formation of liquid phase on firing at relatively low temperature (800-1000 ^oC) which stimulates the densification of the bricks [48].

Table (7): XRF analysis of the raw clay.

Oxides	Wt %
SiO_2	48.735
Al_2O_3	17.72
Fe_2O_3	10.86
TiO_2	1.854
CaO	1.099
MgO	1.987
Na_2O	1.075
K_2O	0.97
P_2O_3	0.205
SO_3	0.021
Cr_2O_3	0.039
MnO	0.039
Cl	0.76
L.O.I	14.5

- **L.O.I: Loss of Ignition.**

3.1.5. Water Content and Plasticity of the raw clay.

Fig (10) shows the relation between the amount of water added to 100 g dry clay material and the deformation ratio L_o / L (on Peffefernkorn apparatus). As clear from Fig (10) average value of the plasticity of the clay attains 48 % (corresponding to L_o / L =2.5-3.3) which means highly plasticity raw clay. That is identified by the high fraction of fine material in the clay. It is needed then to mix the clay batch with sand or any other opening non plastic material to reduce the plasticity or water requirement for clay shaping in the aim of reducing drying problems.

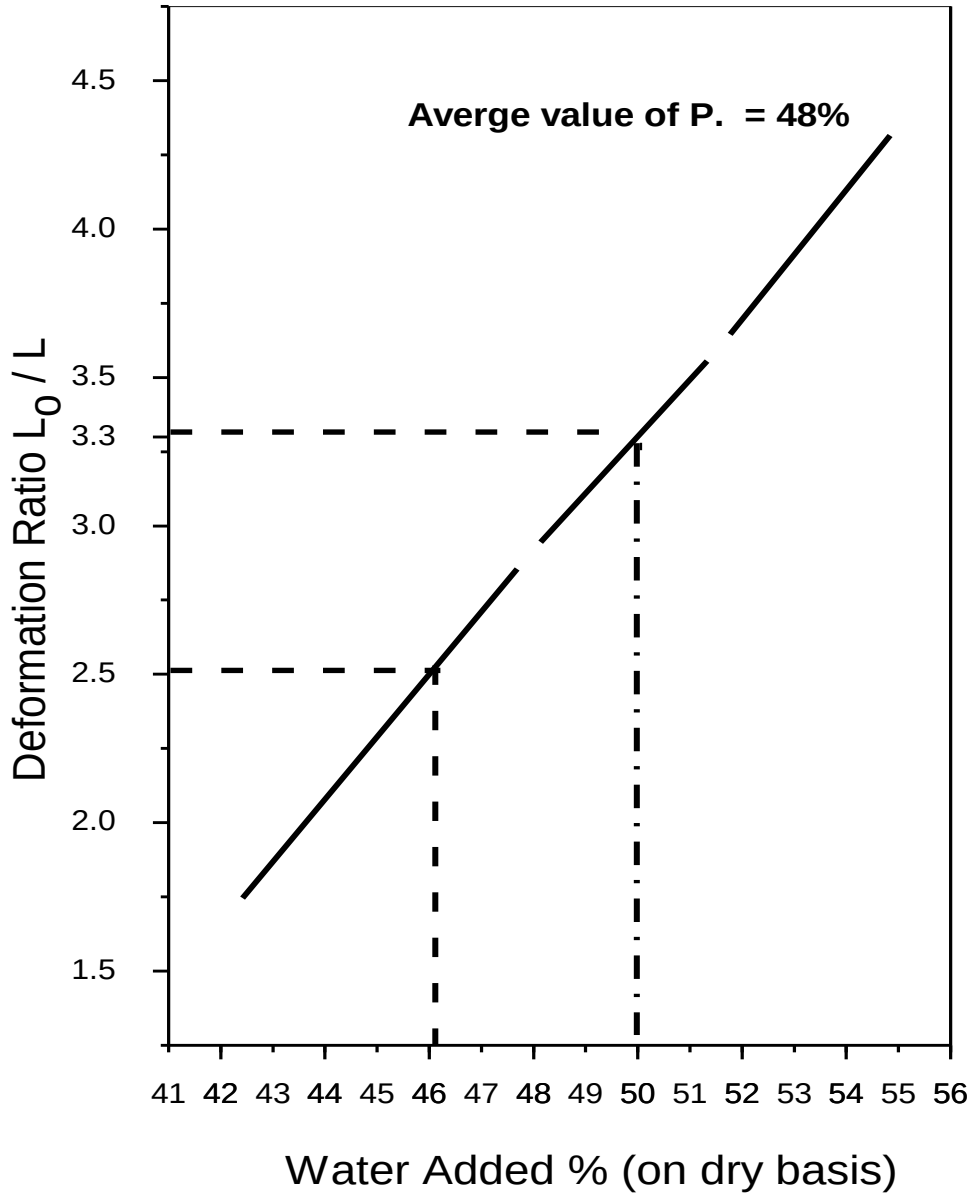

Fig (10): Plasticity curves of the studied raw clay sample according to Pfefferkorn method.

3.1.6. The drying sensitivity (Bigot curve) of the raw clay .

Bigot curve representing the behavior of the extruded clay bricks samples on drying is shown in Fig (11). The latter relates the average linear shrinkage of the brick sample on drying and the water removed expressed as % by weight of the original wet slabs.

As shown from Fig (11), the clay batch is considered highly sensitive to drying referring to the steepness of the curve. Shrinkage attains about 14% of the original brick length; It proceeds till the brick looses about 15% of its original weight as water. This represents the first stage of drying.

Afterwards the shrinkage ceases and drying proceeds till the sample lose its whole water content = 34 % of its original weight. This represents the second stage of drying

In other words, about 44 % of the total water evolved on drying is accompanied by shrinkage where as about 56 % of the water evolves without shrinkage.

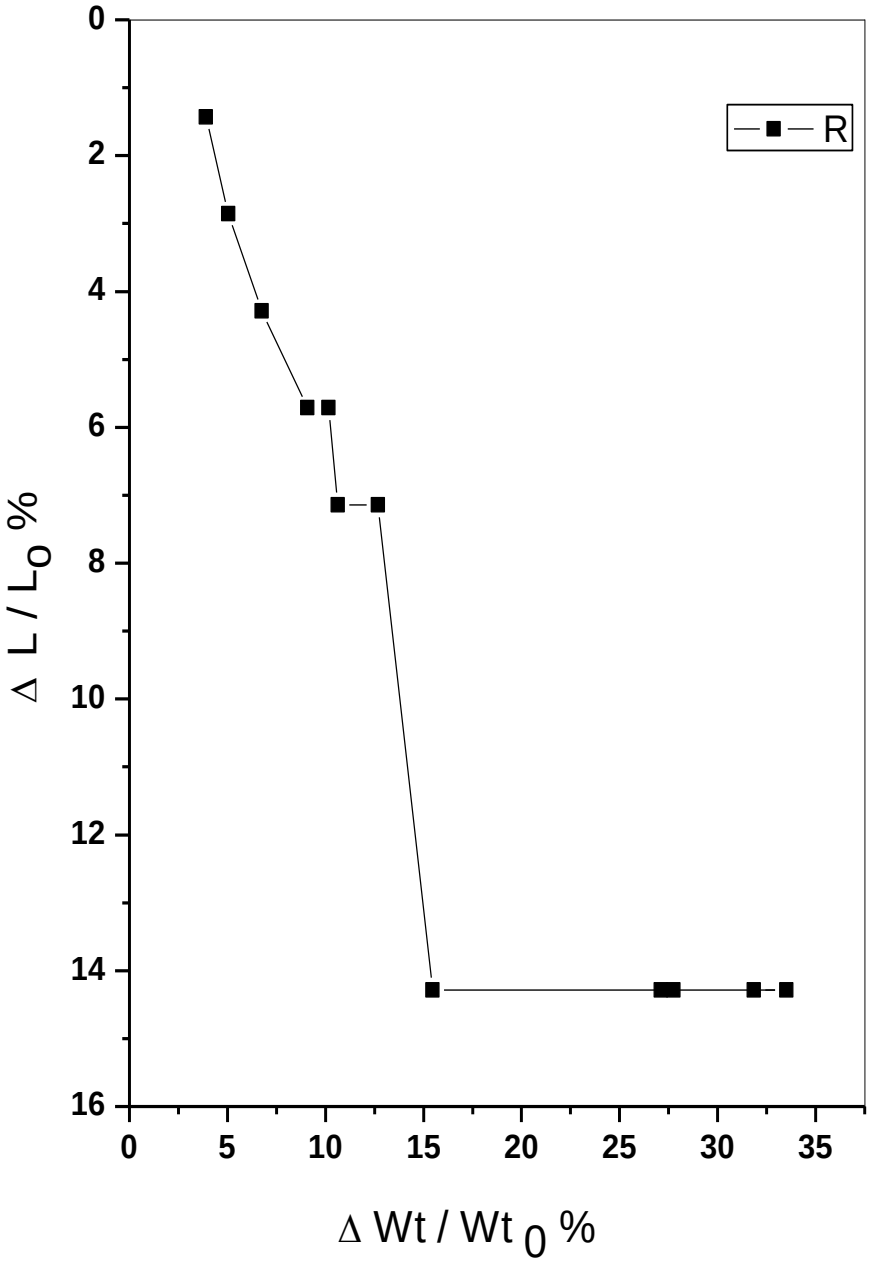

Fig (11): Bigot curve of the raw clay.

3.2. Characterization of the additives.

3.2.1. X-ray diffraction for waste fired clay bricks (Grog)

Fig (12) exhibits the obtained XRD pattern of a waste fired clay bricks rejects. It is evident that low quartz, anothrite $CaAl_2Si_2O_8$ and albite ($NaAlSi_3O_8$) are the main crystalline phases detected in the fired sample. In addition, some XRD lines belonging to hematite (Fe2O3) are shown.

This is mainly attributed to the relatively low firing temperature (~850 ^{0}C). At such temperature, the available CaO, Al_2O_3 and SiO_2 liberated after almost complete dissociation of clay minerals react together to form appreciable amount of anorthite. Meanwhile , most of quartz mineral coexists from due to its lower reactivity at ≈ 850 ^{0}C as compared with the amorphous silica (SiO_2) liberated from the clay minerals structure.

3.2.2. Sieve analysis of used additives

3.2.2.1. Sieve analysis of added sand.

The particle size distribution of the sand was determined by sieve analysis using a sieve set (2, 1.6, 1, 0.6, 0.16 mm).

Table (8): Sieve analysis of sand added.

Size (mm) >	**2**	**1.6**	**1**	**0.6**	**0.16**	**< 0.16>0.063**
%	**13**	**3**	**3.9**	**6.1**	**36**	**38**

The results of the sand sieve analysis as shown in Table (8) show that the fine sand fraction (< 0.16 mm) attains about 38% which is relatively high.

3.2.2.2. Sieve analysis of added saw dust .

The sawdust was taken from the lot at wood-work refuse dump. Wood chips and strands were removed from the sawdust and it was sieve analyzed as shown in Table (9).

Table (9): Sieve analysis of saw dust added.

Size (mm)	**2**	**1.6**	**1**	**0.6**	**0.16**	**< 0.16**
%	**0.8**	**0.5**	**1.6**	**4**	**68.1**	**25**

3.2.2.3. Sieve analysis of added ground waste fired brick (grog)

The fired brick wastes used in this study was brought from Misr Company for building bricks. They were crushed and ground to be divided into two categories.

Category A: fine fraction of particle size ranging from a 0.6-0.3 mm.
Category B: Coarse fraction of particle size ranging from a 2-1.6 mm.

3.3.Effect of additives on the properties of the clay batch :

3.3.1 .Effect on plasticity.

3.3.1.1. Effect of Sand :

As shown from Figs (13), (14) the plasticity of clay batch decreases remarkably with sand additions . Sand as non plastic additives vary from 9.5 - 40% by weight of the clay batch. On addition of 40% sand, the plasticity decearses by about 35% of its original value to reach 31 % .

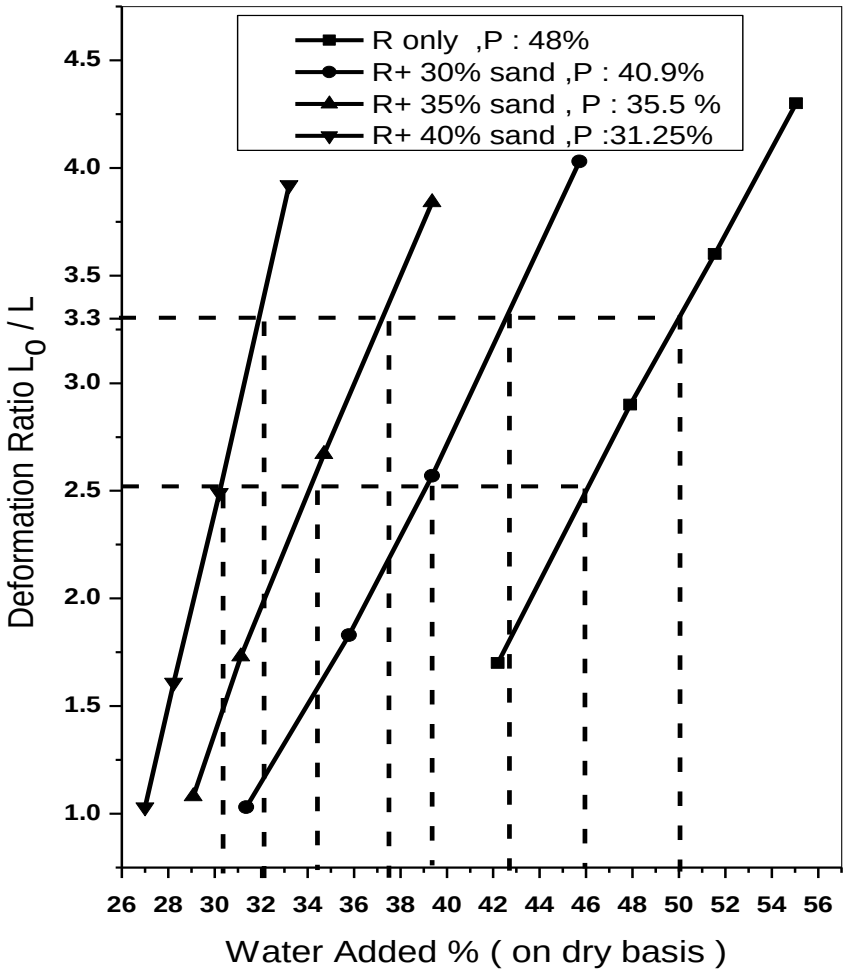

Fig(13): Plasticity curve of the studied raw clay sample with (blank 9.5%, 30%, 35%, 40%) by wt sand according to pfefferkorn method.

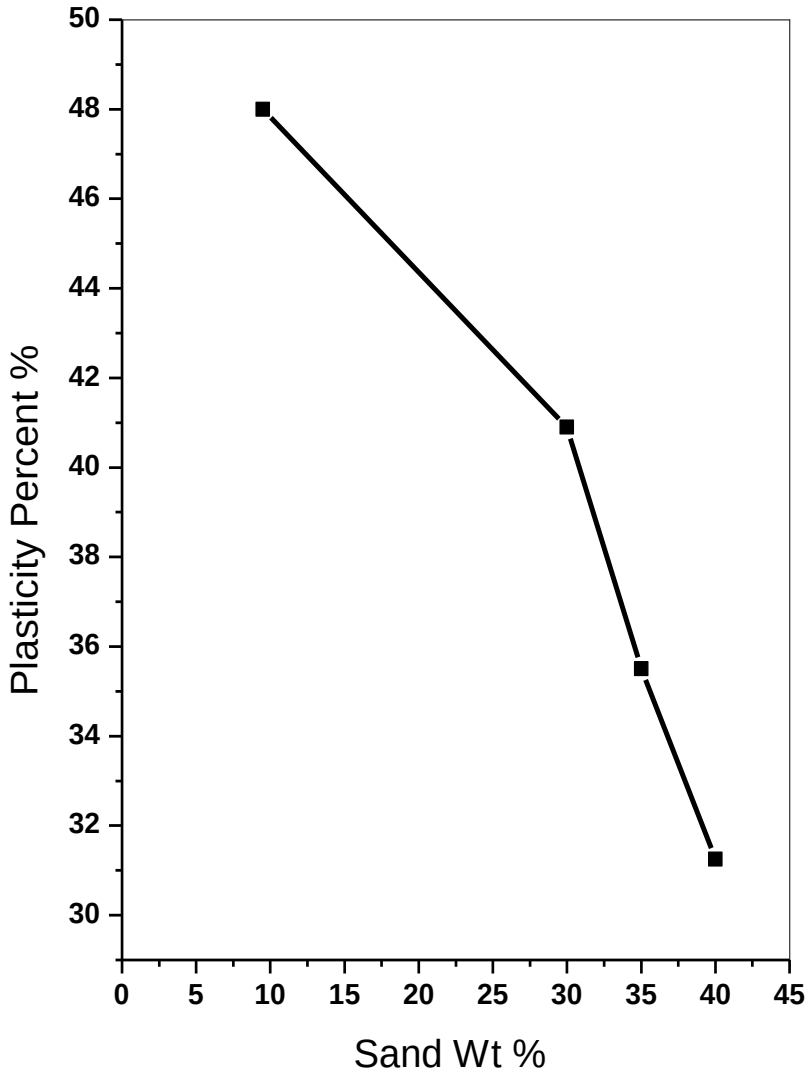

Fig (14): The relation between the plasticity percent and sand additives percent .

3.3.1.2. Effect of Sawdust on plasticity of clay batch .

As shown from Figs (15), (16) the plasticity of the clay batch increases on replacing a part of the sand content in the 40% wt sand batch by 5% and 10% sawdust. The plasticity of the batch increases in presence of saw dust due to its fibrous and water absorbing nature which leads to increase of the water content. On adding 5% and 10% saw dust to the batch the plasticity increases from 31% to 37 % and 42% respectively. But it is still smaller than the raw clay batch without additives (9.5% sand)

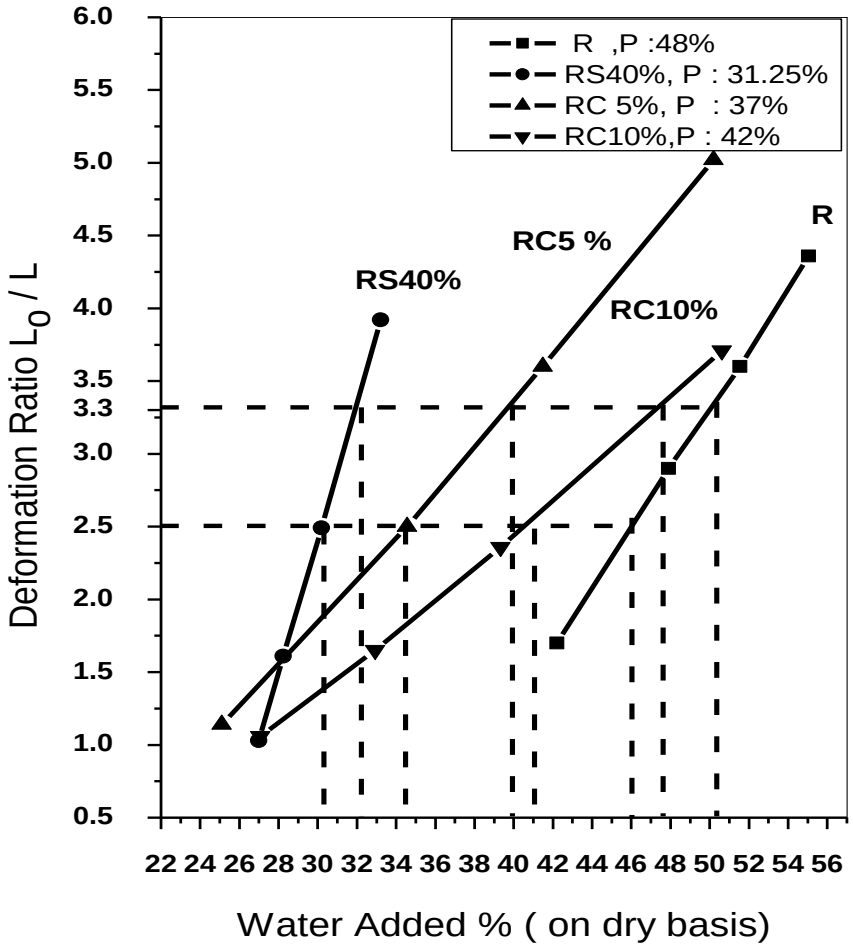

Fig (15): Plasticity curve of the studied raw clay sample with (5%, 10%) by wt sawdust + (35, 30 %) by wt sand according to Pfefferkorn method**.**

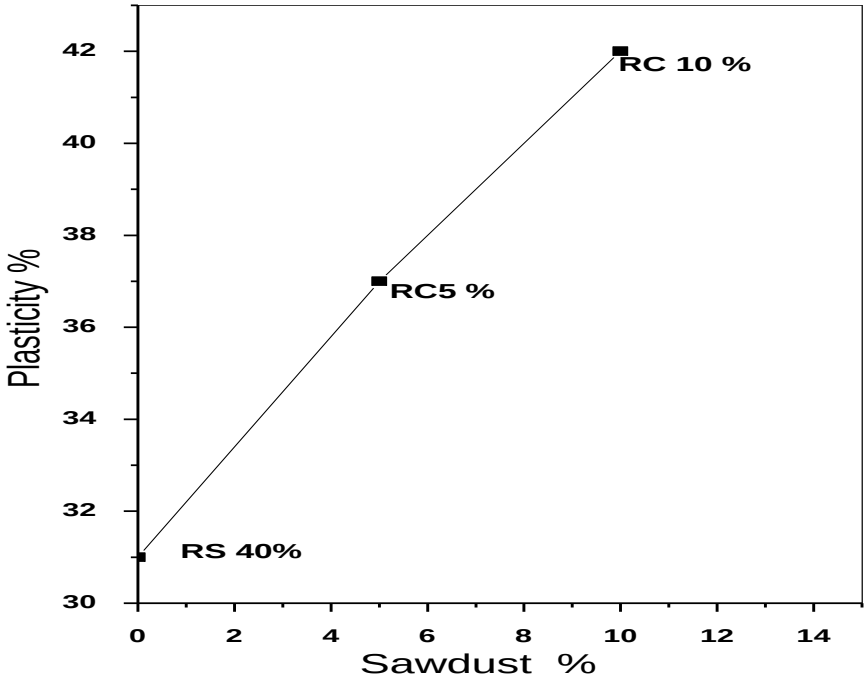

Fig (16): The relation between the plasticity percent and sawdust additives percent.

3.3.1.3. Effect of Fine and Coarse Grog :

As shown from Figs (17), (18) the plasticity of the clay batch decreases with addition of fine grog. It decreases to 33% on addition of 30% grog. The plasticity of the clay batch also decraeses with addition of coarse grog, as shown in Fig (19),(20), it attains 37% on addition of 30% by wt coarse grog. The fine grog has then more considerable effect on decreasing plasticity of the clay batch than coarse grog. That can be attributed to the larger voids fraction and conrsequently the larger water uptake in case of using coarse grog in contrast to the case of using fine grog where smaller voids predominates in the clay batch .

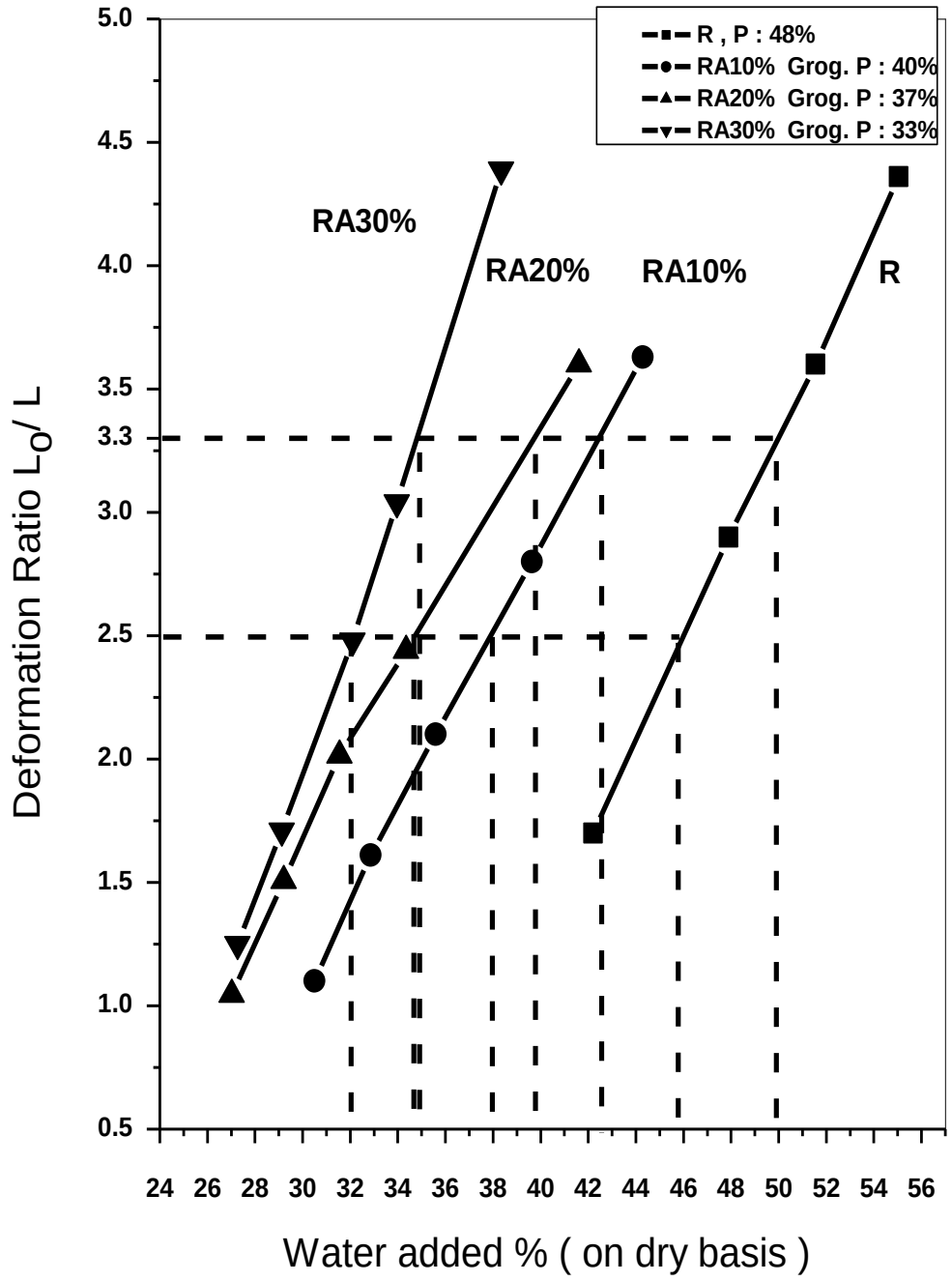

Fig (17): Plasticity curve of the studied raw clay sample with (10%, 20%, 30%) by wt fine grog (0.6-0.3mm) according to Pfefferkorn method.

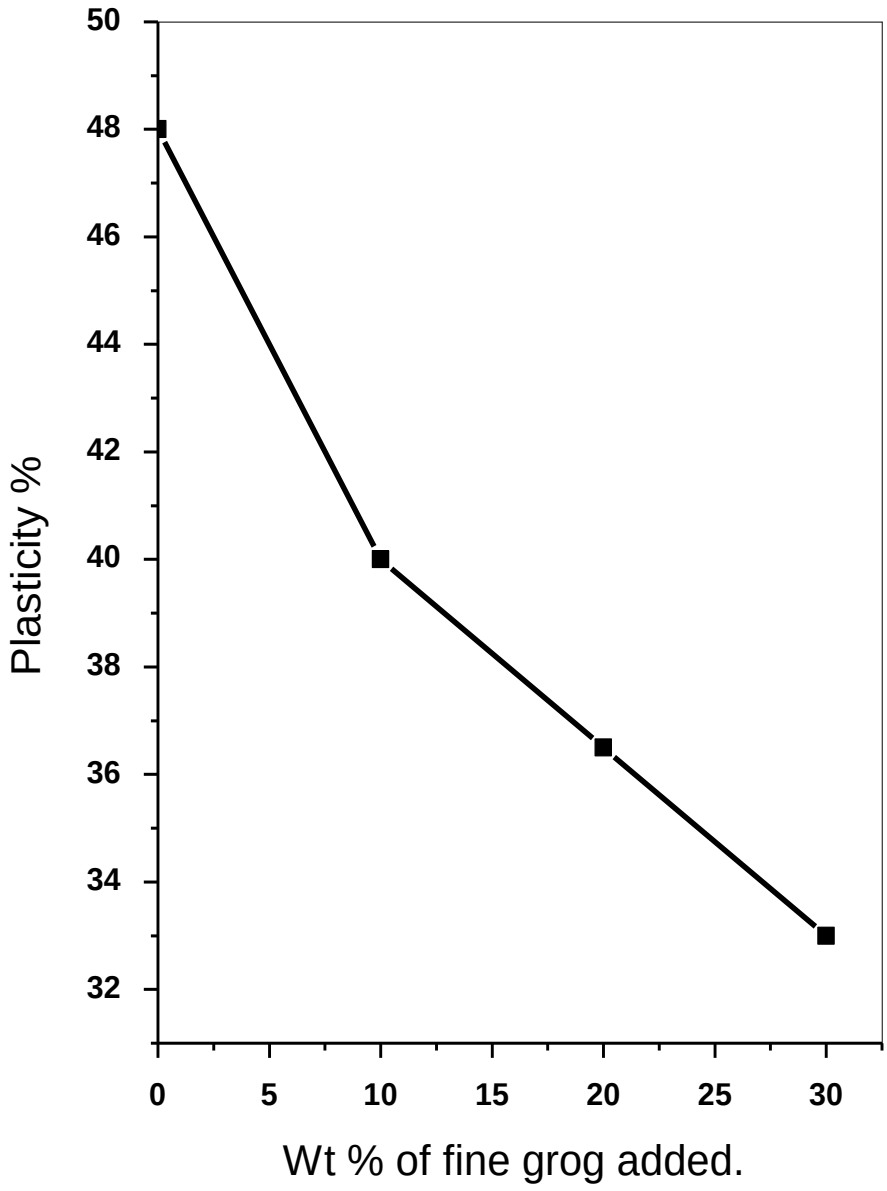

Fig (18): The relation between the plasticity percent and fine grog additives percent.

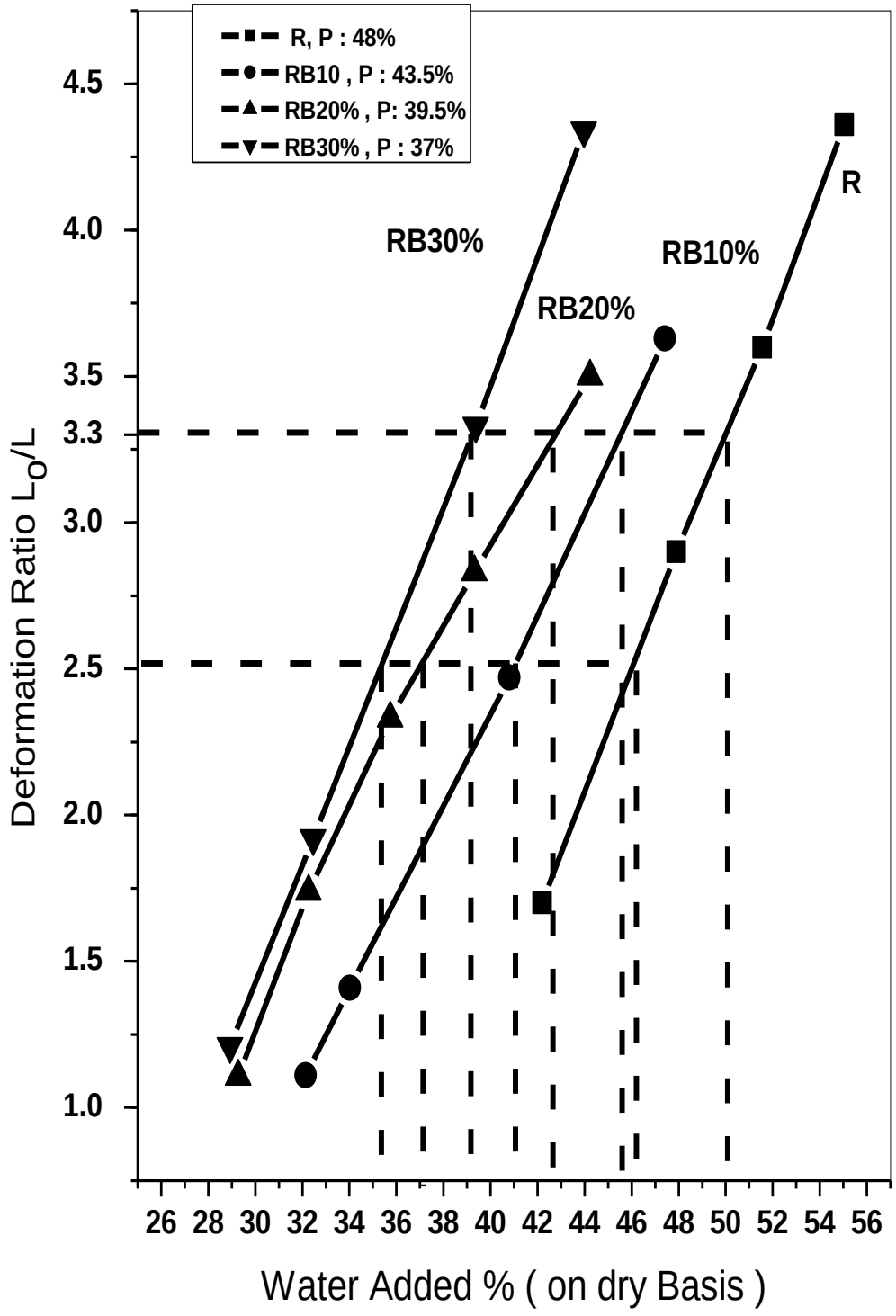

Fig (19): Plasticity curve of the studied raw clay sample with (10%, 20%, 30%) by wt coarse grog (2-1.6 mm) according to Pfefferkorn method.

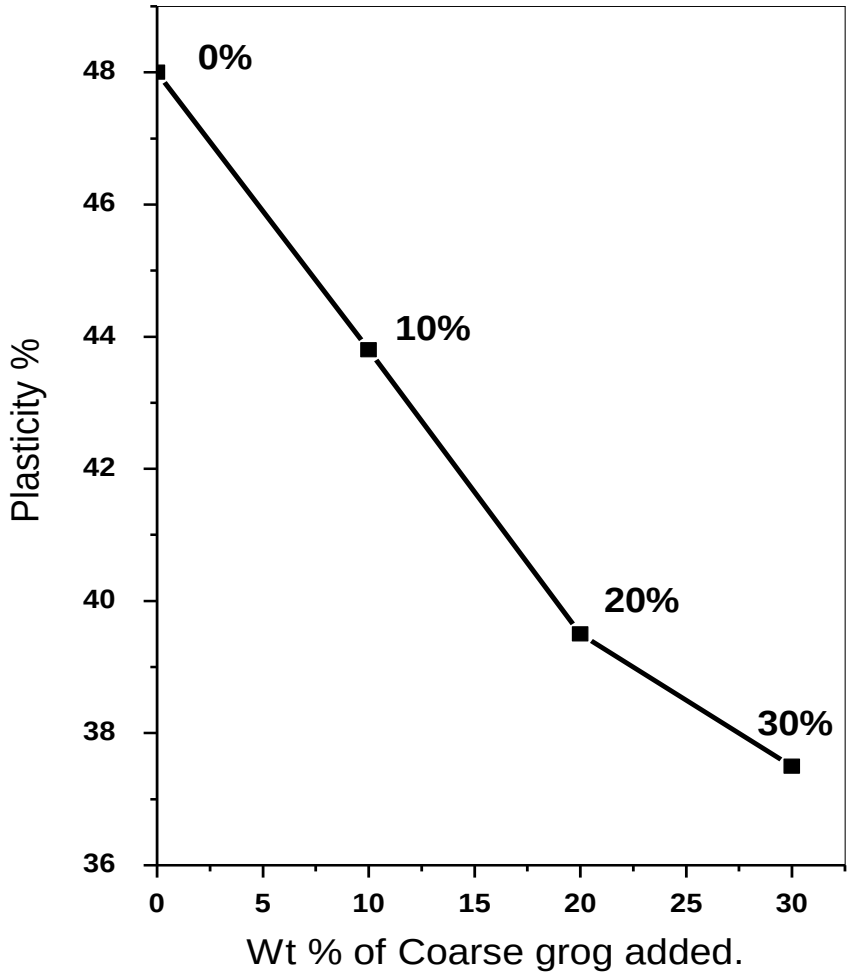

Fig (20): The relation between the plasticity percent and coarse grog additives percent.

The effect of all the stuidied additives on the plasticity of the raw clay are summarized in Table (10) and Fig (21).

Table (10): The plasticity of prepared batches .

Symbol	Type of additives	Plasticity %
R	Blank	48%
RS 40%	40% Sand	30.25%
RA10%	10% Fine Grog	40%
RA20%	20% Fine Grog	37%
RA30%	30% Fine Grog	33%
RB10%	10% Coarse Grog	43.5%
RB20%	20% Coarse Grog	39.5%
RB30%	30% Coarse Grog	37%
RC 5%	5% Sawdust+35% Sand	37%
RD 10%	10% Sawdust+30% Sand	43%

From the results shown in Table (10) it is clear that the plasticity decraeses with increasing the non- plastic additives percent in the clay batch such as sand and grog (fine, coarse) .From the values of clay batch plasticity as shown in Table (10) and Fig (21), it is clear that the realively low plasticity value can be attained through addition of 40% sand or 30% fine bricks rejects or 5% saw dust + 35% sand to the raw clay. The plasticity value corresponding to the latter addition is the highest one but that can be compensated through the reinforcement effect of the sawdust givinig highly strength to the dry bricks. In addtition liberation of heating value of saw dust in the firing kiln would result in fuel saving.

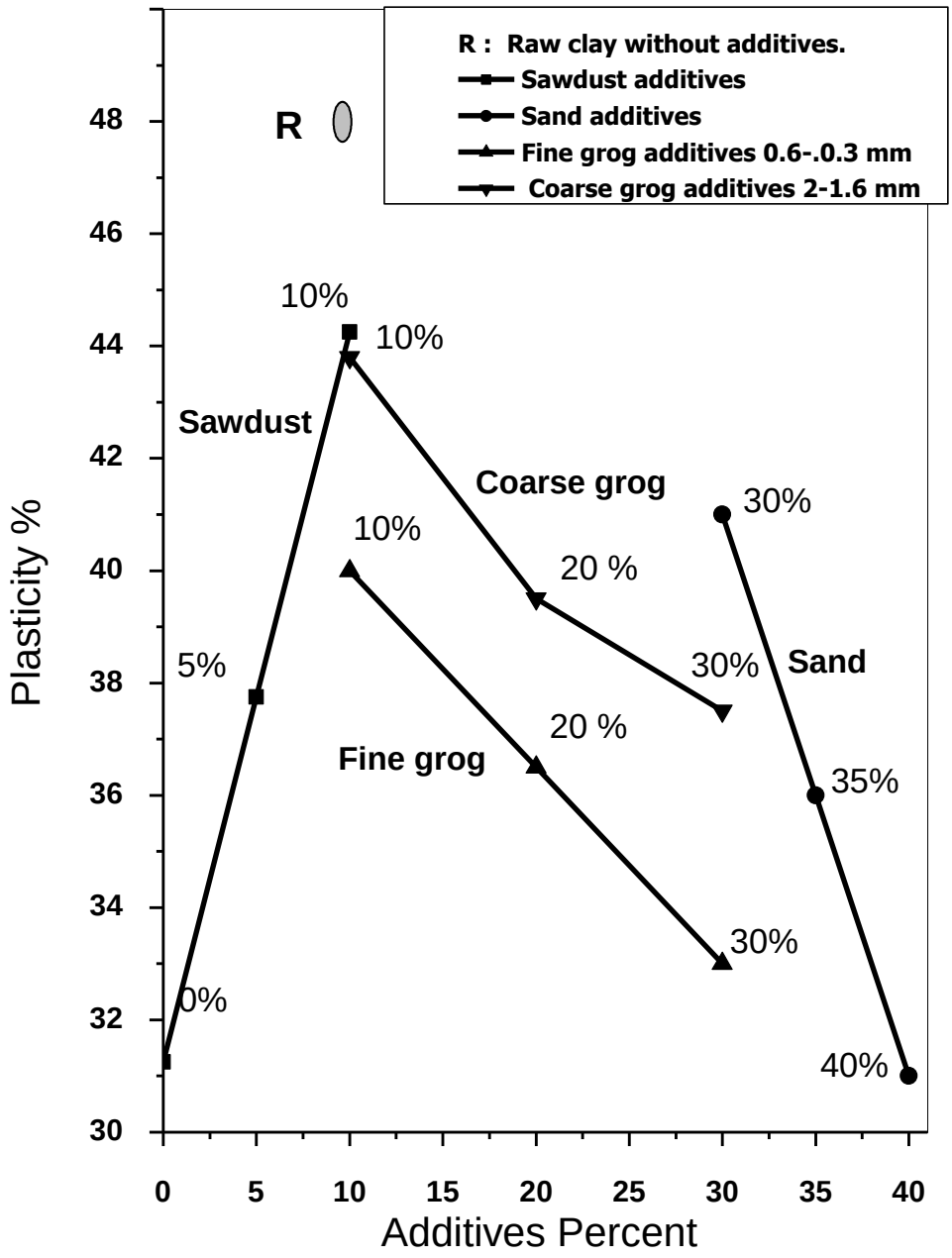

Fig (21): Effect of various additives on the plasticity of the raw clay batch .

3.3.2. Effect of additives on drying sensitivity (Bigot Curve) of the raw clay.

3.3.2.1. Effect of the sand.

Fig (22) shows the Bigot curve (drying shrinkage curve) of the raw clay batch and of that contain 40 % sand. Comparing the two curves, it's clear that drying sensitivity of the clay batch was highly improved thorough addition of the sand.

In case of the batch with 40% sand shrinkage attains about 7 % of the original brick length; Shrinkage proceeds till the brick looses about 10 % of its original weight as water. In other words, about 33% of the total water evolved on drying is a accompanied by shrinkage. Afterwards the 2 nd phase of drying begins and proceeds till it loses its whole water content (= 30.25% of its original weight).

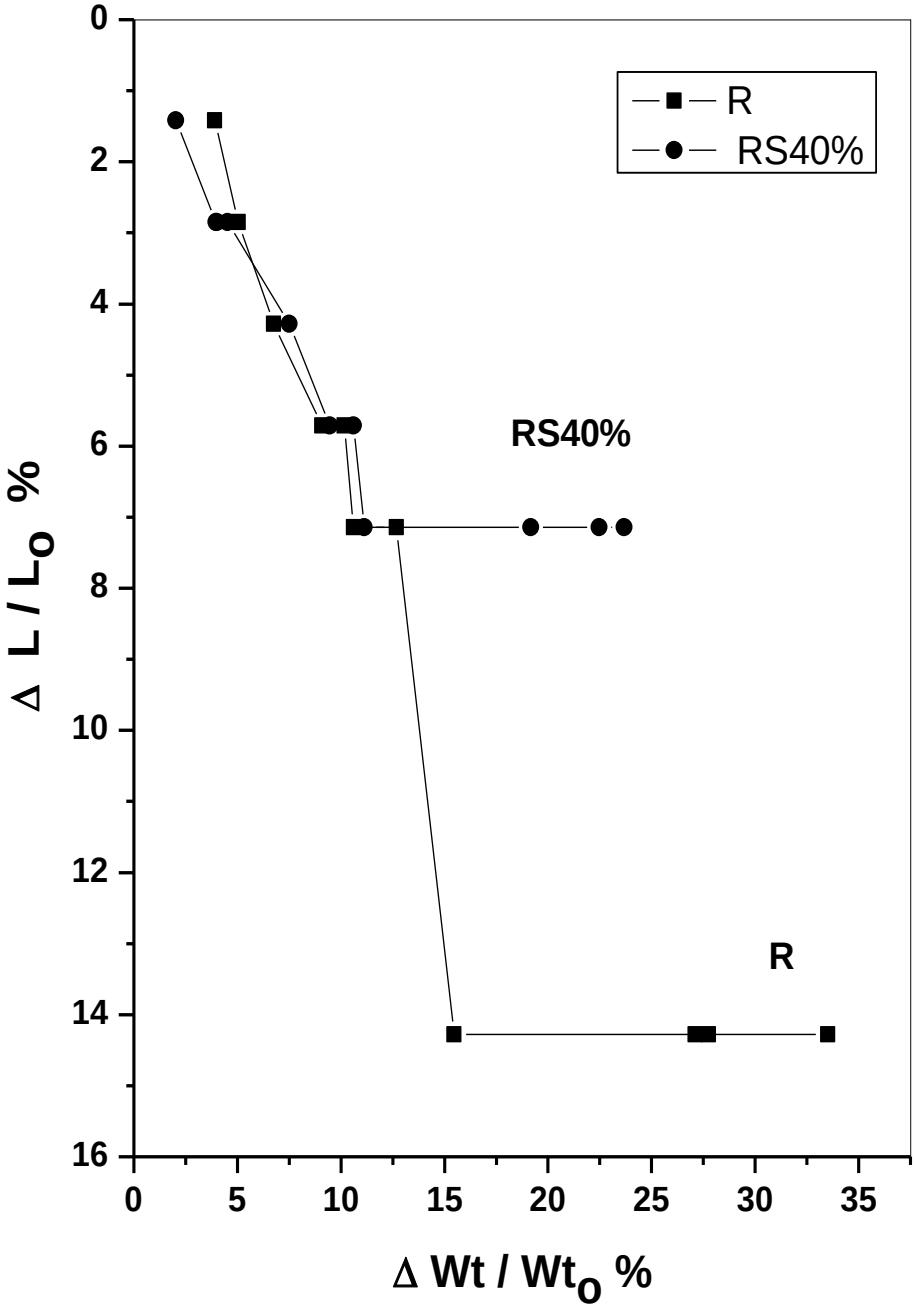

Fig (22): Effect of sand additive on Bigot curve of the clay batch .

3.3.2.2. Effect of the fine grog additives.

Fig (23) shows the drying shrinkage (Bigot curve) of the clay batch without additive and with 10, 20, 30 wt % fine grog ; As show from Fig (23) the drying sensitivity of the clay batch, represented by the steepness of the slope of the shrinkage curve and the amount of drying shrinkage decreases with addition of the fine grog.

For clay batch with 30 % fine grog shrinkage attains about 8.5 % of the original brick length, the brick looses about 10 % of its original weight as water. In other words, about 30% of the total water evolved on drying is accompanied with shrinkage where as about 70 % of the water evolved without shrinkage. Afterwards the 2 nd phase of drying begins and proceeds till it loses its whole water content (=33 % of its original weight).

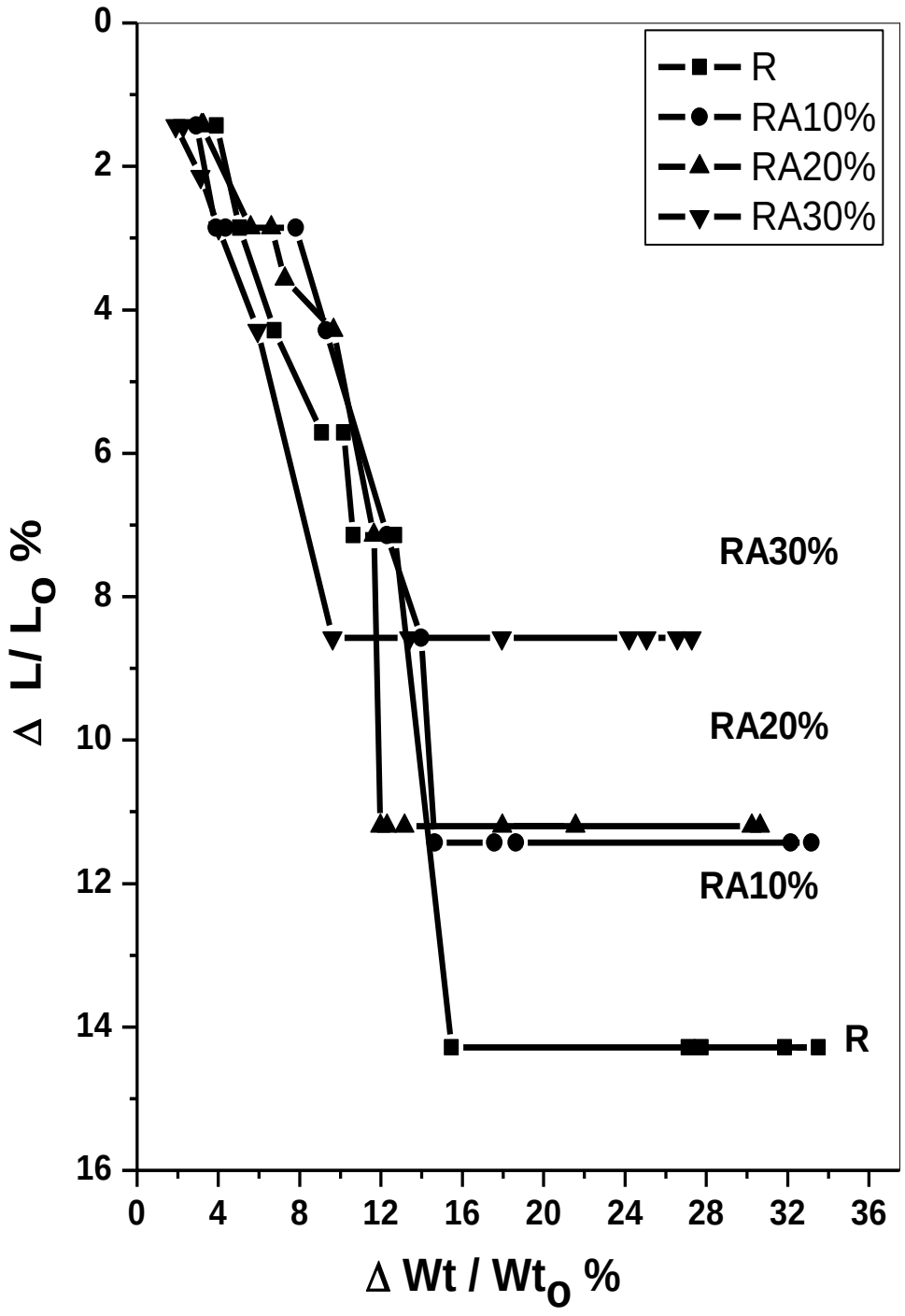

Fig (23): Effect of fine grog additive on Bigot curve of the clay batches.

3.3.2.3. Effect of the coarse grog additives.

As shown from the Fig (24) the coarse grog batch RB30% Shrinkage attains about 9.5 % of the original brick length, the brick looses about 11 % of its original weight as water. In other words, about 29 % of the total water evolved on drying is accompanied with shrinkage where as about 71 % of the water evolved without shrinkage. Afterwards the 2 nd phase of drying begins and proceeds till it loses its whole water content (=37 % of its original weight).

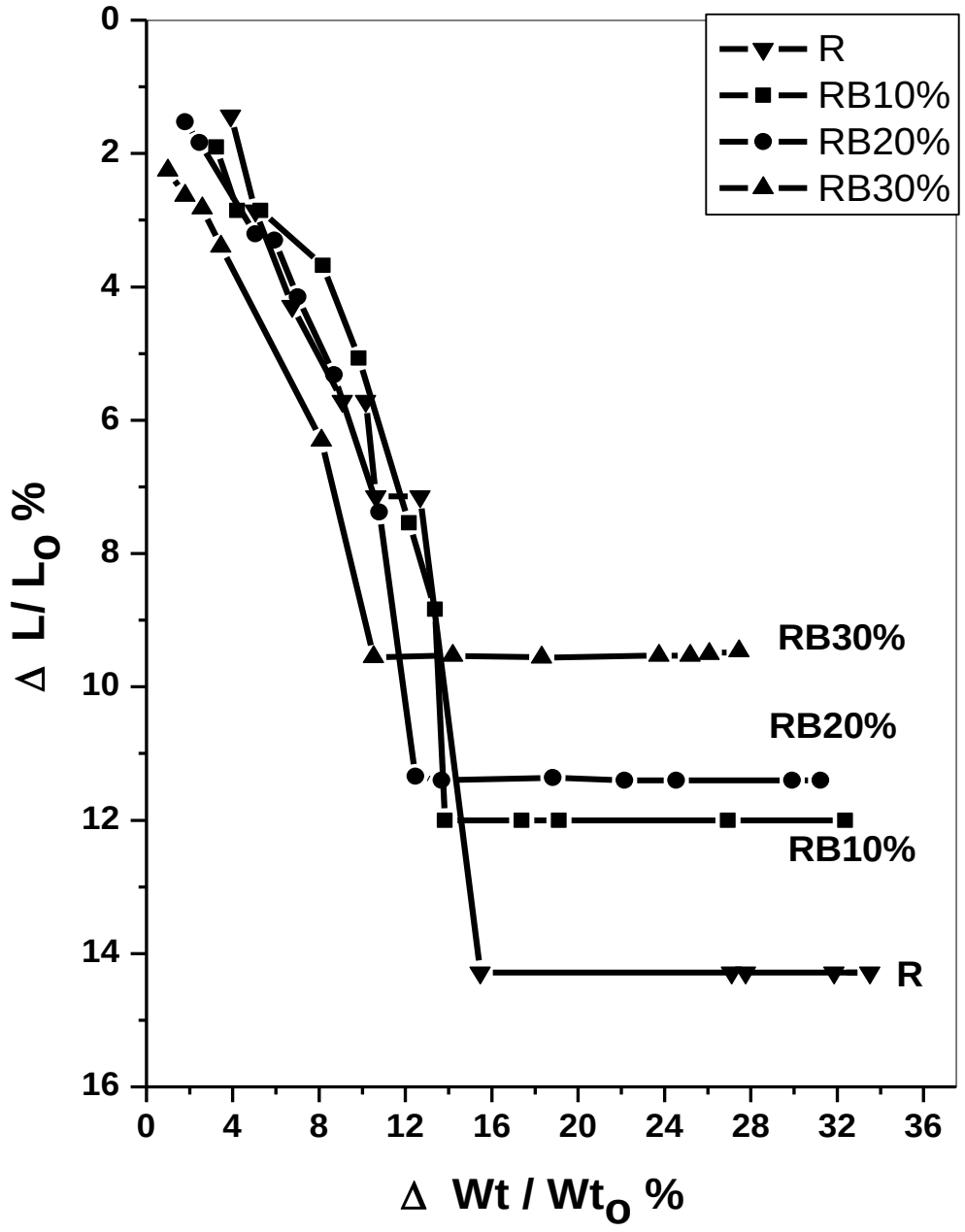

Fig (24): Effect of coarse grog additive on Bigot curve of the clay batches.

3.3.2.4. Effect of saw dust addition.

As shown from the Fig (25) the sawdust batch RC5% Shrinkage attains about 7 % of the original brick length, the brick looses about 15 % of its original weight as water. In other words, about 29 % of the total water evolved on drying is a accompanied with shrinkage where as about 71 % of the water evolved without shrinkage. Afterwards the 2 nd phase of drying begins and proceeds till it loses its whole water content (=37 % of its original weight). For the sawdust batch RC10% Shrinkage attains about 8.5 % of the original brick length, the brick looses about 21 % of its original weight as water. In other words, about 49 % of the total water evolved on drying is a accompanied with shrinkage where as about 51 % of the water evolved without shrinkage. Afterwards the 2 nd phase of drying begins and proceeds till it loses its whole water content (= 43 % of its original weight).

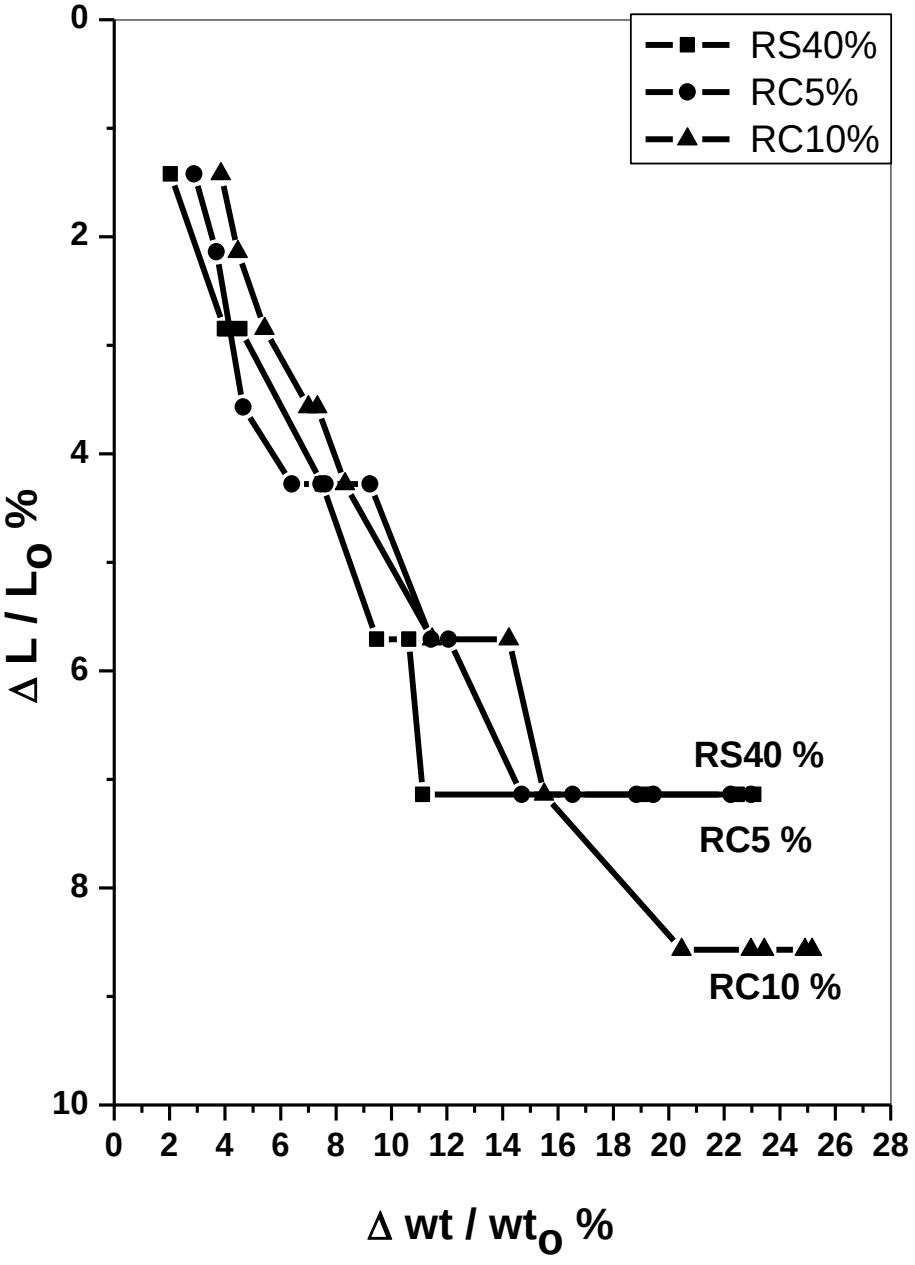

Fig (25): Effect of saw dust additions on Bigot curve of the clay batches.

3.4. Effect of additives on the physico mechanical properties of fired brick samples .

3.4.1. The total linear shrinkage.

The values of the total linear shrinkage of the samples against percentage of additives, sand, sawdust and grog, as function of the firing temperatures were illustrated extensively.

3.4.1.1. Effect of sand.

Table (11) and Figure (26) show the change of the total linear shrinkage of brick samples with sand content and with firing temperatures.

As show from Table (11), the total linear shrinkage of the brick sample decreases remarkably with increase of sand content in the batch. From Fig (26) it is clear that, the total linear shrinkage increases with increase of firing temperature for all batches.

Table (11): The total linear shrinkage of (R, RS40%) batches fired samples.

Symbol	Total linear shrinkage %			
	750 ^{o}C	800 ^{o}C	850 ^{o}C	Additives type
R	9.63	10.36	10.84	Blank
RS40%	7.4	7.85	8.1	Sand addition

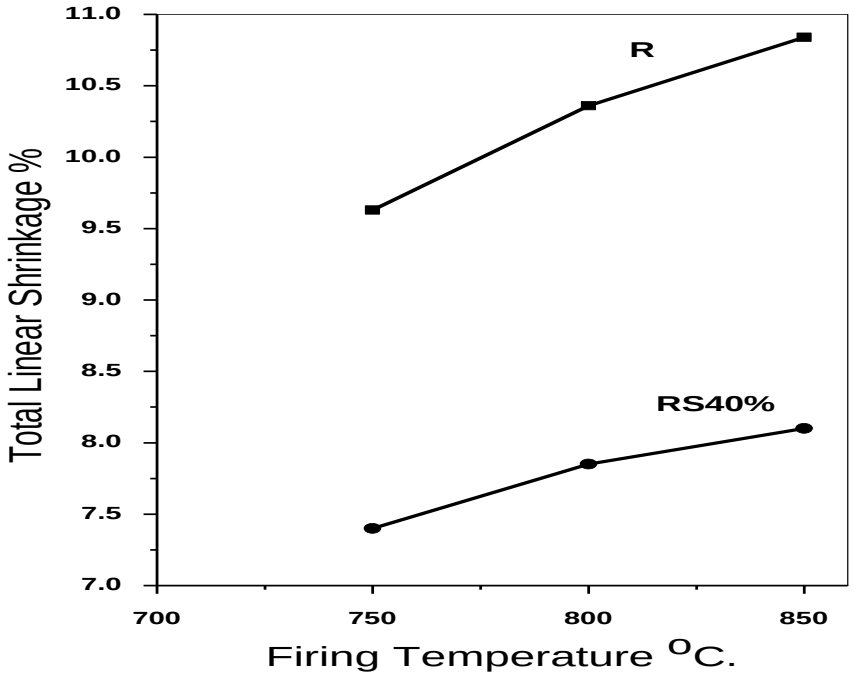

Fig (26): The relation between the total linear shrinkag and firing temperatures as funcation of % sand additives.

3.4.1.2. Effect of Saw dust.

Figures (27, 28) show the change of total linear shrinkage of brick samples with saw dust content and with firing temperature respectively.

As shown from Figure (27) the total linear shrinkage increases with increase of saw dust (as replacement to sand) for all firing temperature. From Figure (28) it is clear that, the total linear shrinkage increases with increase of firing temperature for all batches, but in all cases the total linear shrinkage is still far less than that of the raw clay specimen .

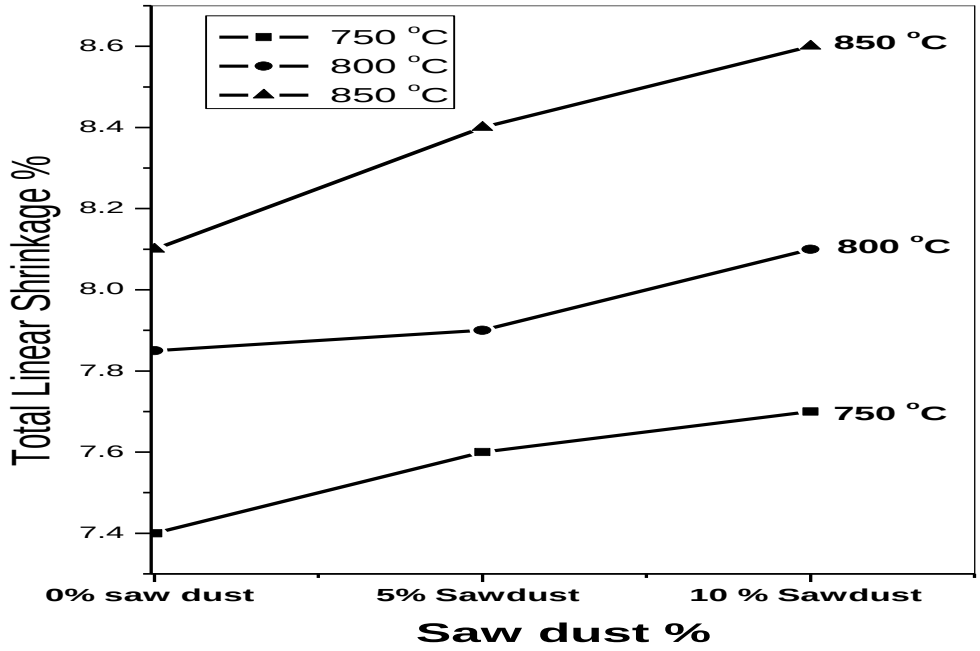

Fig (27): The relation between the linear shrinkag and saw dust additives percent.

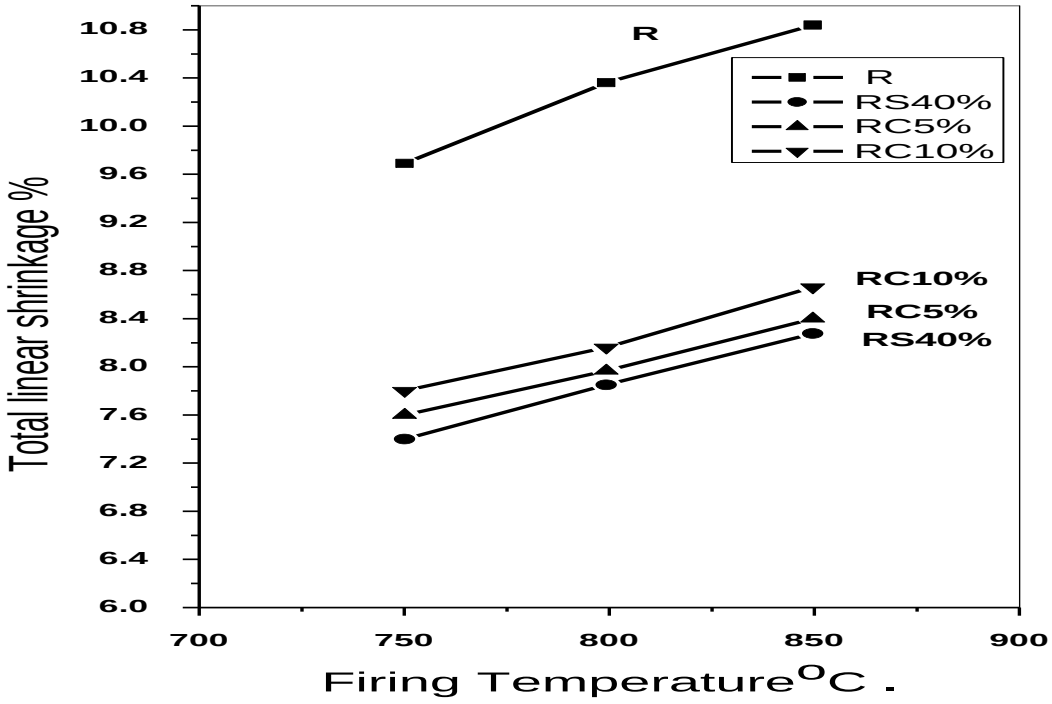

Fig (28): The relation between the total linear shrinkag and saw dust additives with firing temperatures.

3.4.1.3. Effect of fine and coarse waste fired bricks (Grog).

Figures (29, 30) show the total linear shrinkage of brick samples with fine grog content and with firing temperatures respectively.

As shown from Figure (29) the total linear shrinkage of the brick samples decreases remarkably with increase of fine grog content in the batches. From Figure (30) it is clear that, the total linear shrinkage increases with increase of firing temperatures for all batches.

Figures (31, 32) show the total linear shrinkage of brick samples with coarse grog content and with firing temperatures respectively.

As shown from Figure (31) the total linear shrinkage of the brick samples decreases remarkably with increase of coarse grog content in the batches. From Figure (32) it is clear that, the total linear shrinkage increases with increase of firing temperatures for all batches. From Figures (29-32) it is clear that, the coarse grog addition has more considerable effect on the total linear shrinkage than fine grog addition.

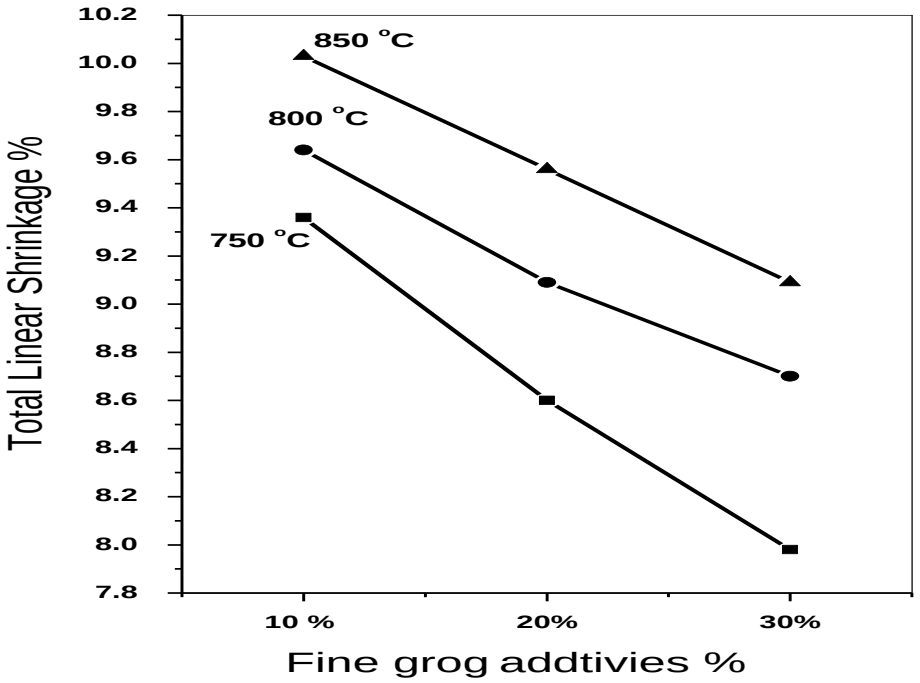

Fig (29): The relation between the linear shrinkag and fine grog additives percent

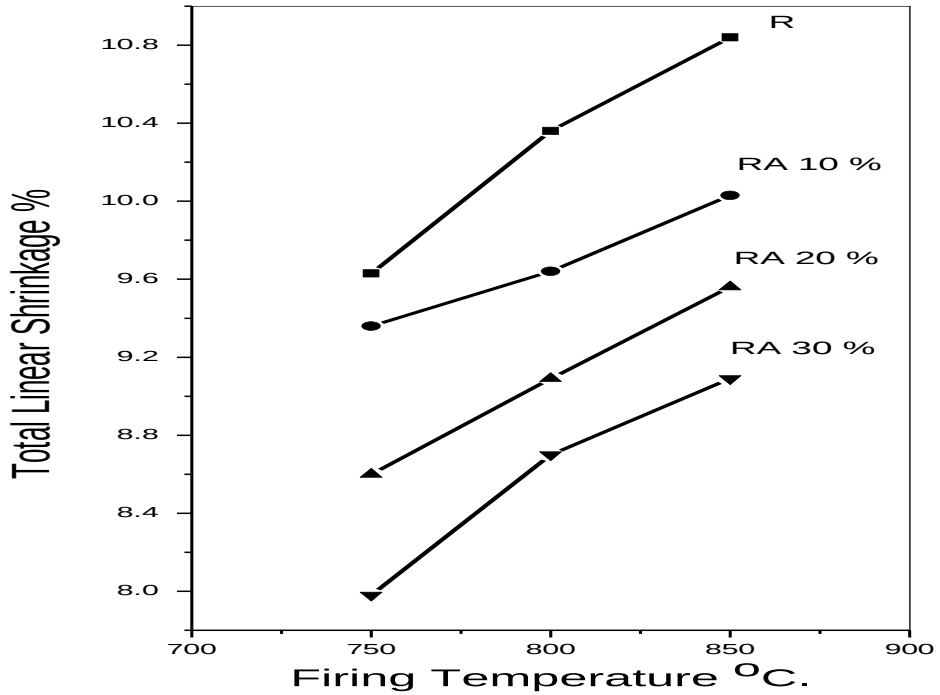

Fig (30): The relation between the linear shrinkag and fine grog additives with firing temperatures.

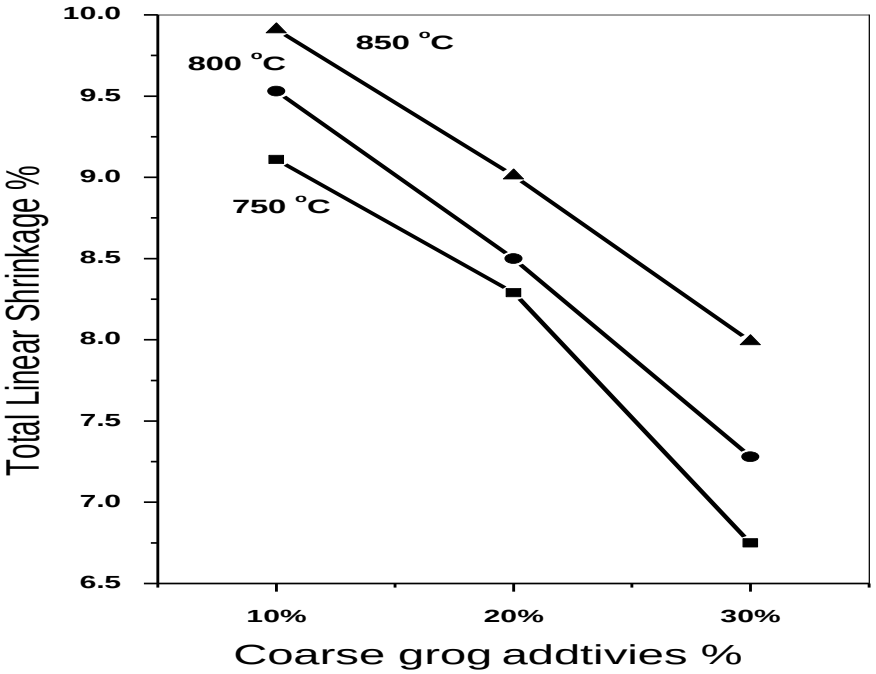

Fig (31): The relation between the linear shrinkag and coarse grog additives percent .

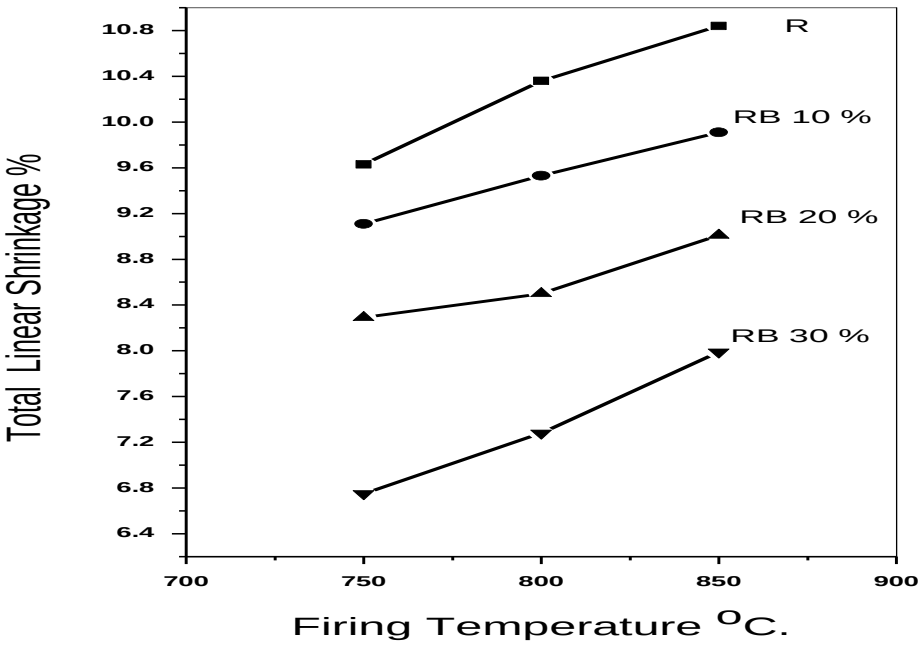

Fig (32): The relation between the linear shrinkag and firing temperatures with coarse grog additives.

Table (12) summarizes the results of the total linear shrinkage of the brick samples with various percentages of studied additives (sand, grog, saw dust) and with firing temperatures.

Table (12): The total linear shrinkage of fired samples with various additives type.

Symbol	Total linear shrinkage %			
	750 ^{o}C	800 ^{o}C	850 ^{o}C	Additives type
R	9.63	10.36	10.84	Blank
RS40%	7.4	7.85	8.1	Sand addition
RA10%	9.36	9.64	10.03	Fine grog addition
RA20%	8.6	9.09	9.56	
RA30%	7.98	8.70	9.09	
RB10%	9.11	9.53	9.91	Coarse grog addition
RB20%	8.29	8.50	9.01	
RB30%	6.75	7.28	7.99	
RC5%	7.6	7.9	8.4	Sawdust addition
RC10%	7.7	8.1	8.6	

From Table (12) it is clear that, all the studied additives leads to more or less comparable values for the decrease of the total linear shrinkage. However the most effective additive on the total linear shrinkage is 30% coarse grog. This can be attributed to large voids fraction attained in case of coarse grog.

3.4.2. The loss on weight on firing.

The values of the loss on weight of the fired samples against percentage of additives, sand, sawdust and grog, as function of the firing temperatures were illustrated extensively.

3.4.2.1. Effect of sand.

Table (13) and Figure (33) show the change of the loss on weight of the fired samples with sand content and with firing temperatures respectively.

As show from Table (13), the loss on weight of the fired samples decreases remarkably with increase of sand content in the batch. From Fig (33) it is clear that, the loss on weight of the fired samples increases with increase of firing temperature for all batches.

Table (13): The loss on weight of raw clay and 40% sand .

Symbol	Loss on Weight , %			
	750 ^{o}C	800 ^{o}C	850 ^{o}C	Additives type
R	8.069	9.41	9.71	Blank
RS40%	4.5	4.8	5.1	Sand addition

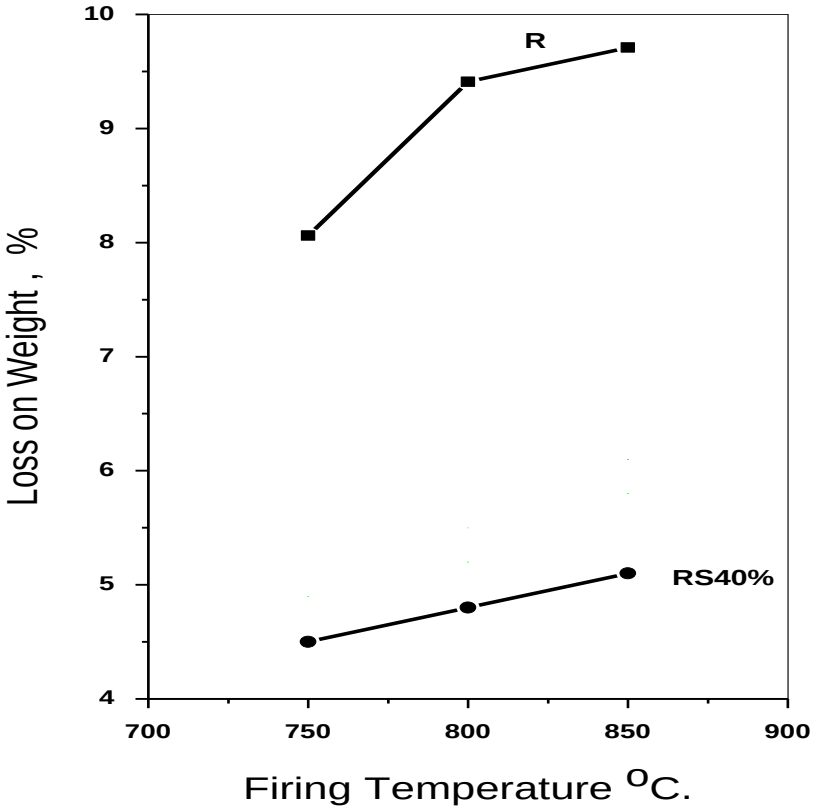

Fig (33): The relation between the loss on weight with sand additives and firing temperatures .

3.4.2.2. Effect of Saw dust.

Figures (34, 35) show the change of the loss on weight of the fired samples with saw dust content and with firing temperature respectively.

As shown from Figure (34) the loss on weight of the fired samples increases with increase of saw dust (as replacement to sand) for all firing temperature. From Figure (35) it is clear that, the loss on weight of the fired samples increases with increase of firing temperatures for all batches, but in all cases the loss on weight of the fired samples is still far less than of the raw clay specimen.

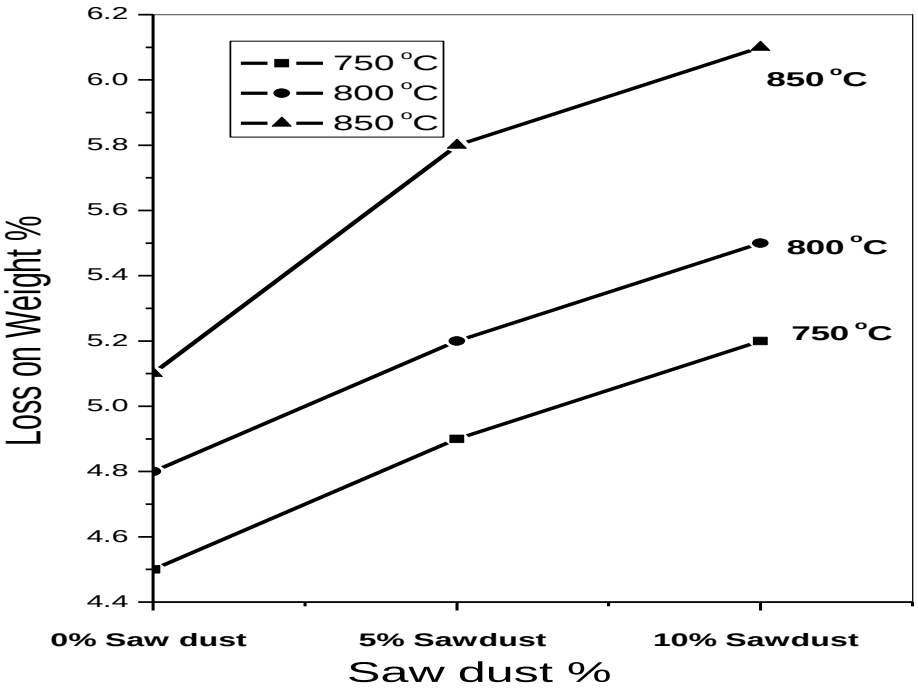

Fig (34): The relation between the loss on weight with the percentage of saw dust additives.

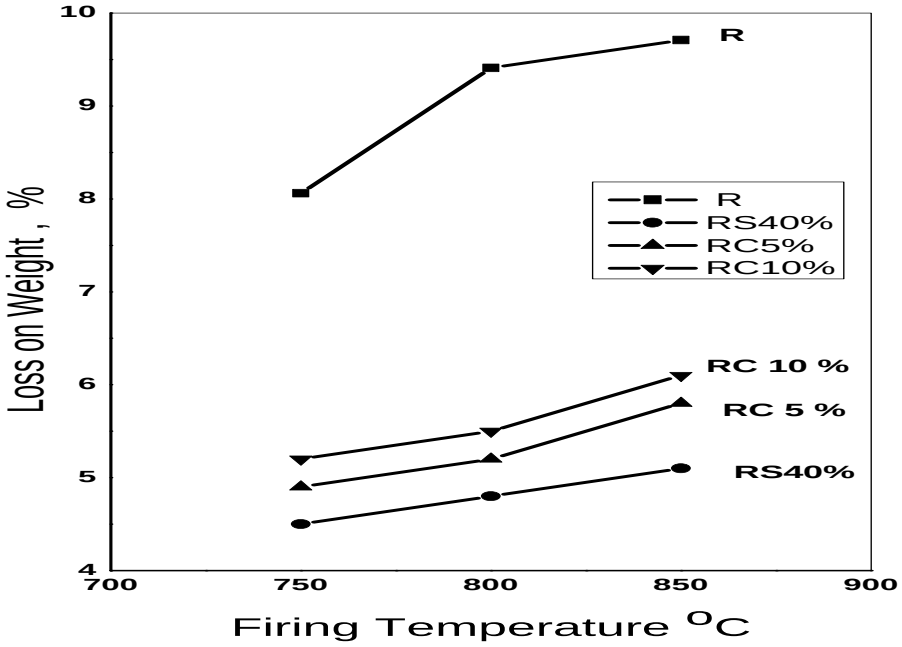

Fig (35): The relation between the loss on weight with saw dust additives and firing temperatures .

3.4.2.3. Effect of fine and coarse Waste fired bricks (Grog).

Figures (36, 37) show the loss on weight of the fired samples with fine grog content and with firing temperatures respectively.

As shown from Figure (36) the loss on weight of the fired samples decreases remarkably with increase of fine grog content in the batches. From Figure (37) it is clear that, the loss on weight of the fired samples increases with increase of firing temperatures for all batches.

Figures (38, 39) show the loss on weight of the fired samples with coarse grog content and with firing temperatures respectively.

As shown from Figure (38) the loss on weight of the fired samples decreases remarkably with increase of coarse grog content in the batches. From Figure (39) it is clear that, the loss on weight of the fired samples increases with increase of firing temperatures for all batches. From Figures (36-39) it is clear that, the coarse grog addition has more considerable effect on the loss on weight of the fired samples than fine grog addition.

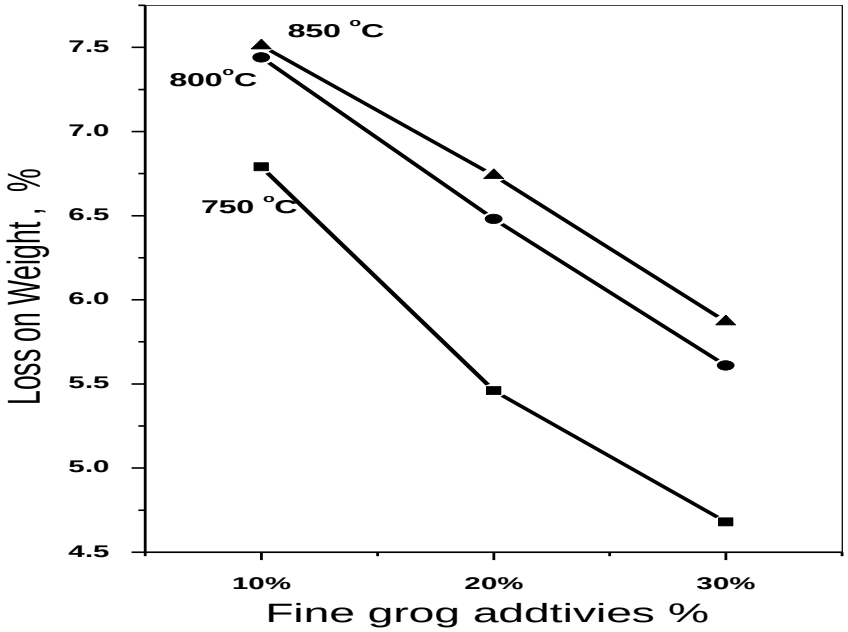

Fig (36): The relation between the loss on weight and fine grog additives percent .

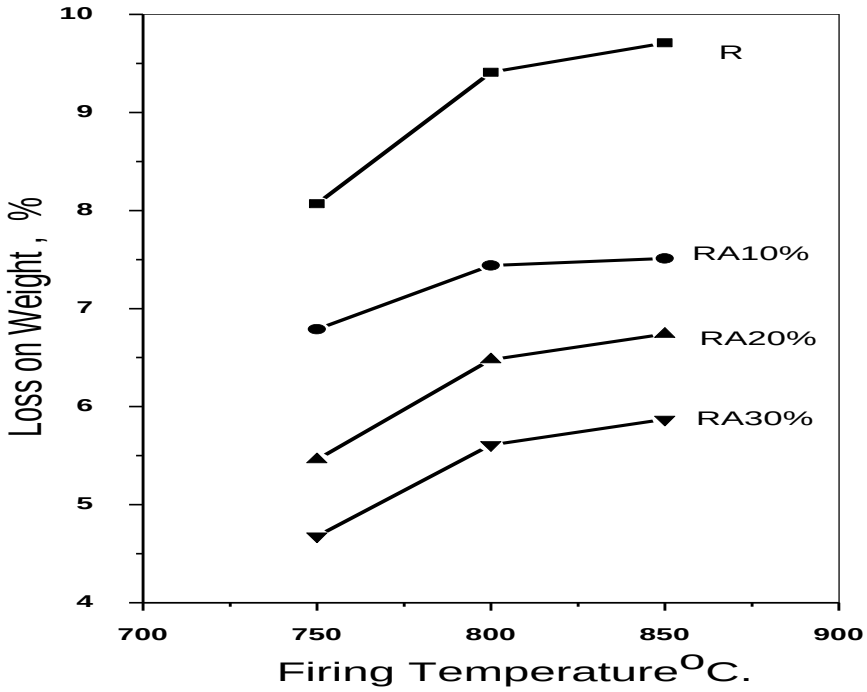

Fig (37): The relation between the loss on weight with fine grog additives and firing temperatures.

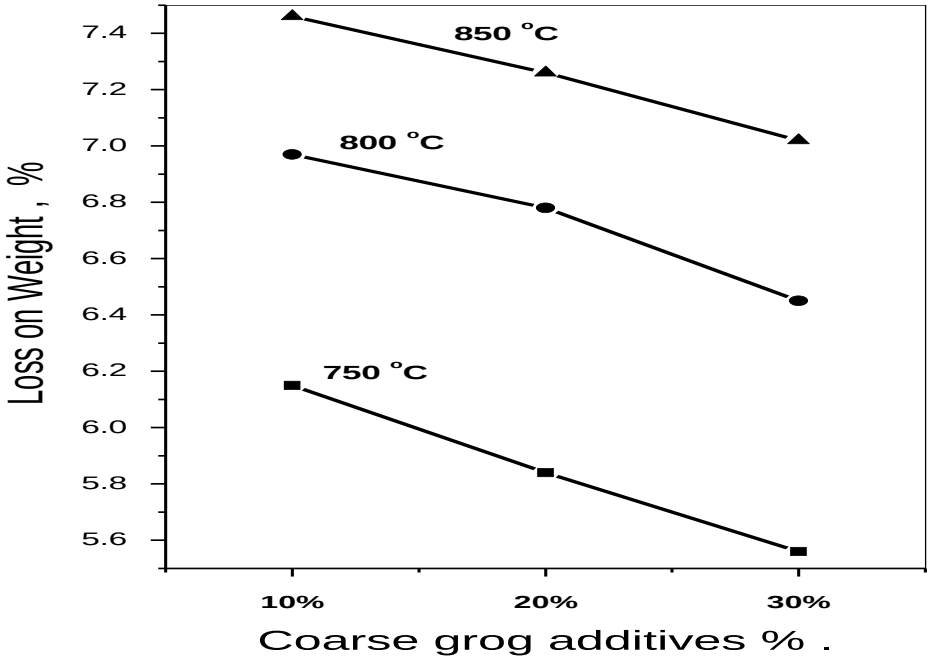

Fig (38): The relation between the loss on weight with coarse grog additives percent .

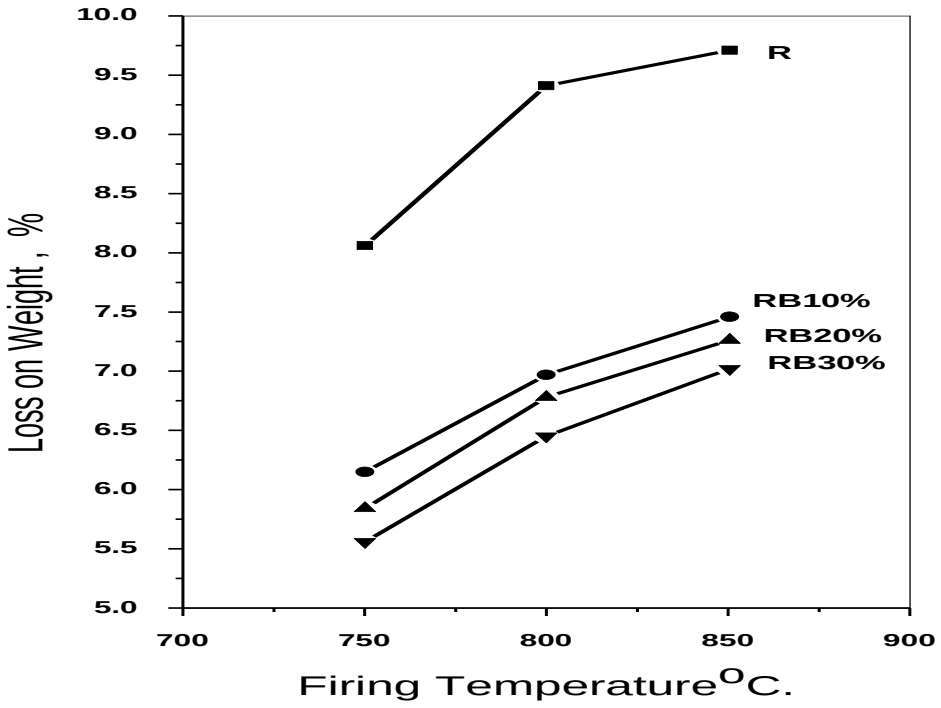

Fig (39): The relation between the loss on weight with coarse grog addition and firing temperatures .

Table (14) summarizes the results of the loss on weight of fired samples with various percentages of studied additives (sand, grog, saw dust) and with firing temperatures.

Table (14): The loss on weight of fired samples

Symbol	Loss on Weight , %			
	750 ^{o}C	800 ^{o}C	850 ^{o}C	Additives type
R	8.069	9.41	9.71	Blank
RS40%	4.5	4.8	5.1	Sand addition
RA10%	6.79	7.44	7.51	Fine grog addition
RA20%	5.46	6.48	6.74	
RA30%	4.68	5.61	5.87	
RB10%	6.15	6.97	7.46	Coarse grog addition
RB20%	5.84	6.78	7.26	
RB30%	5.56	6.45	7.02	
RC5%	4.9	5.2	5.8	Sawdust addition
RC10%	5.2	5.5	6.1	

From Table (14) it is clear that all the studied additives lead to more or less comparable values for the decrease of the loss on weight. However the most effective additives on the loss on weight is 40% sand addition. This can be attributed to that sand and grog have no or very slight loss on weight. Sawdust in contrast has some increasing effect on the L.O.I due to its combustion and change to gaseous products as $CO_2$and H_2O.

3.4.3. The water absorption.

The values of the water absorption of the fired samples against percentage of additives, sand, sawdust and grog, as function of the firing temperatures were illustrated extensively.

3.4.3.1. Effect of Sand.

Table (15) and Figure (40) show the change of the water absorption of the fired samples with sand content and with firing temperatures respectively.

As show from Table (15), the water absorption of the fired samples increases remarkably with increase of sand content in the batch. From Fig (40) it is clear that, the water absorption of the fired samples decreases with increase of firing temperature for all batches.

Table (15): The water absorption of (R, RS40%) fired samples.

Symbol	Water Absorption %			
	750 ^{o}C	800 ^{o}C	850 ^{o}C	Additives type
R	13.49	12.23	12.00	Blank
RS40%	16.8	16.47	16.26	Sand addition

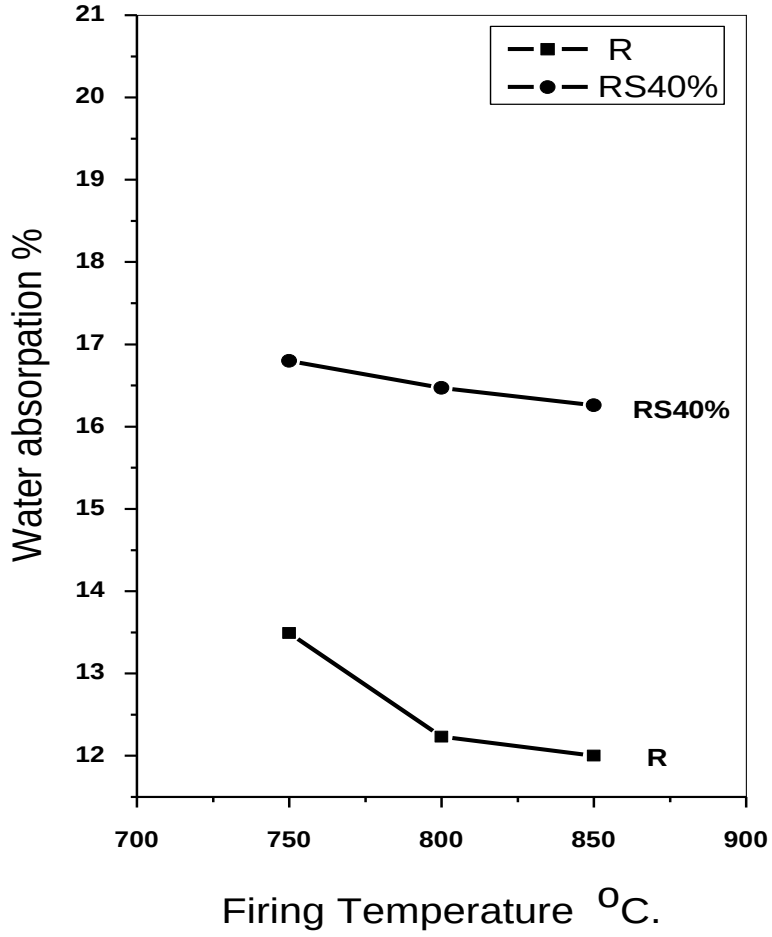

Fig (40): The relation between the water absorption and sand additives with firing temperatures .

3.4.3.2. Effect of Saw dust.

Figures (41, 42) show the change of the water absorption of the fired samples with saw dust content (as replacement to 40% sand) and with firing temperature respectively.

As shown from Figure (41) the water absorption of the fired samples increases with increase of saw dust for all firing temperature. From Figure (42) it is clear that, the water absorption of the fired samples decreases with increase of firing temperatures for all batches.

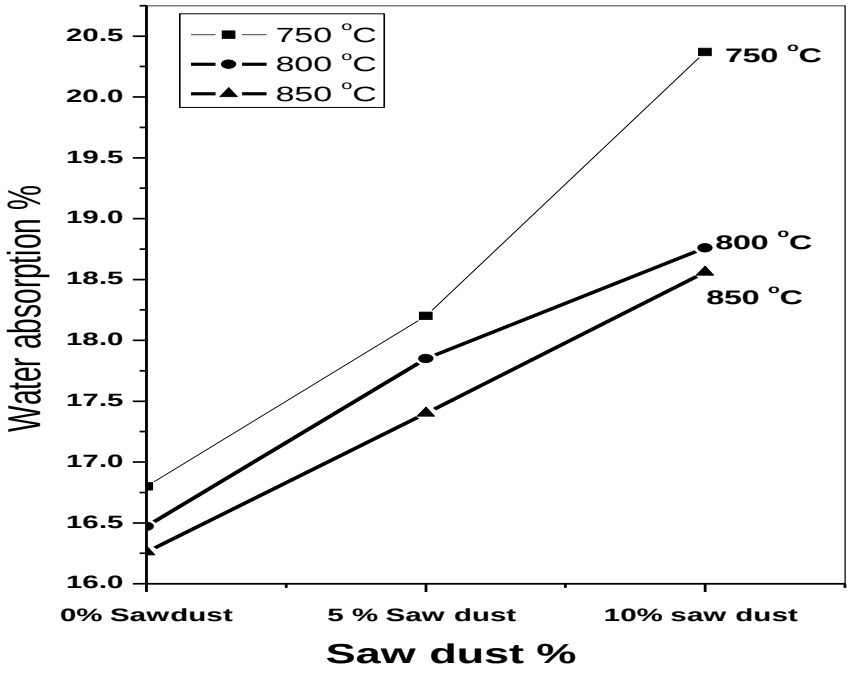

Fig (41): The relation between the water absorption and sand, saw dust additives with firing temperature .

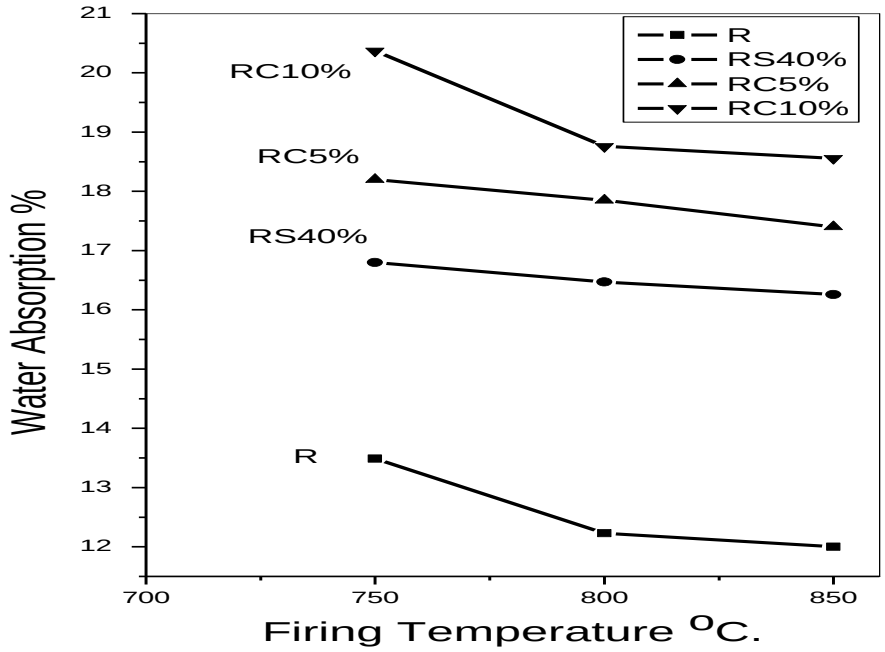

Fig (42): The relation between the water absorption and sand, saw dust additives with firing temperatures .

3.4.3.3. Effect of fine and coarse waste fired bricks (Grog).

Figures (43, 44) show the water absorption of the fired samples with fine grog content and with firing temperatures respectively.

As shown from Figure (43) the water absorption of the fired samples increases remarkably with increase of fine grog content in the batches. From Figure (44) it is clear that, the water absorption of the fired samples decreases with increase of firing temperatures for all batches.

Figures (45, 46) show the water absorption of the fired samples with coarse grog content and with firing temperatures respectively.

As shown from Figure (45) the water absorption of the fired samples increases remarkably with increase of coarse grog content in the batches. From Figure (46) it is clear that, the water absorption of the fired samples decreases with increase of firing temperatures for all batches. From Figures (43-46) it is clear that, the coarse grog addition has more considerable effect on the water absorption of the fired samples than fine grog

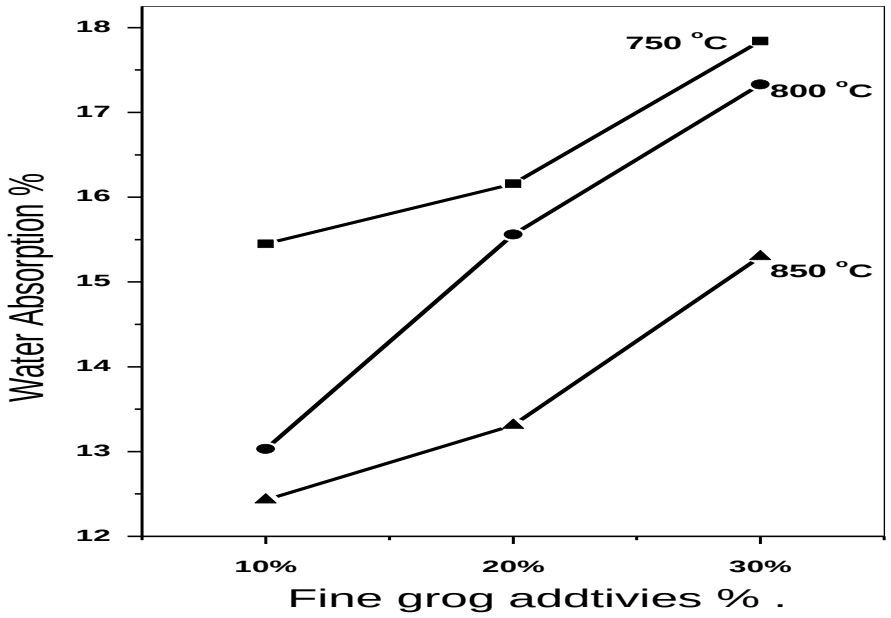

Fig (43): The relation between the water absorption and fine grog additives percent .

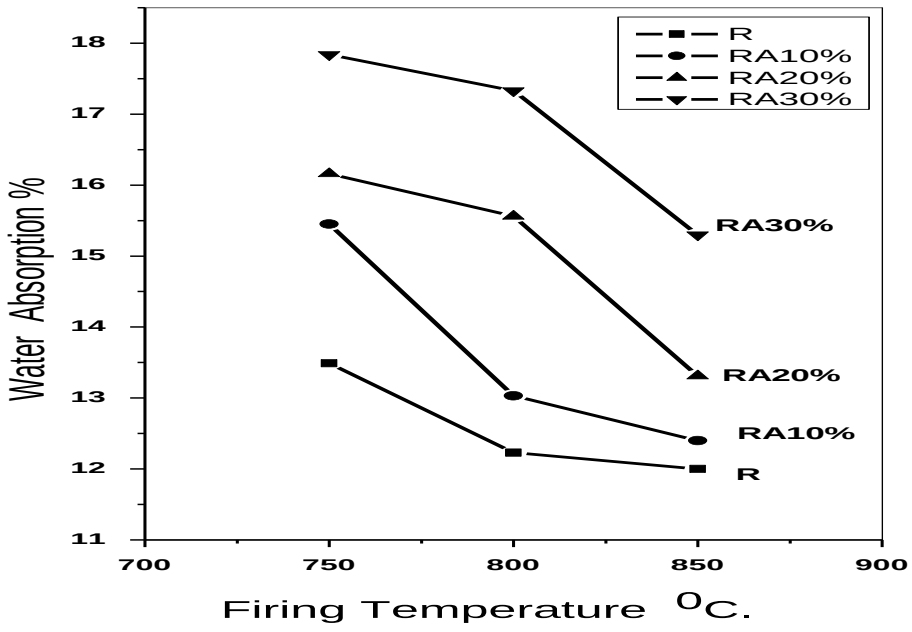

Fig (44): The relation between the water absorption and fine grog additives with firing temperatures .

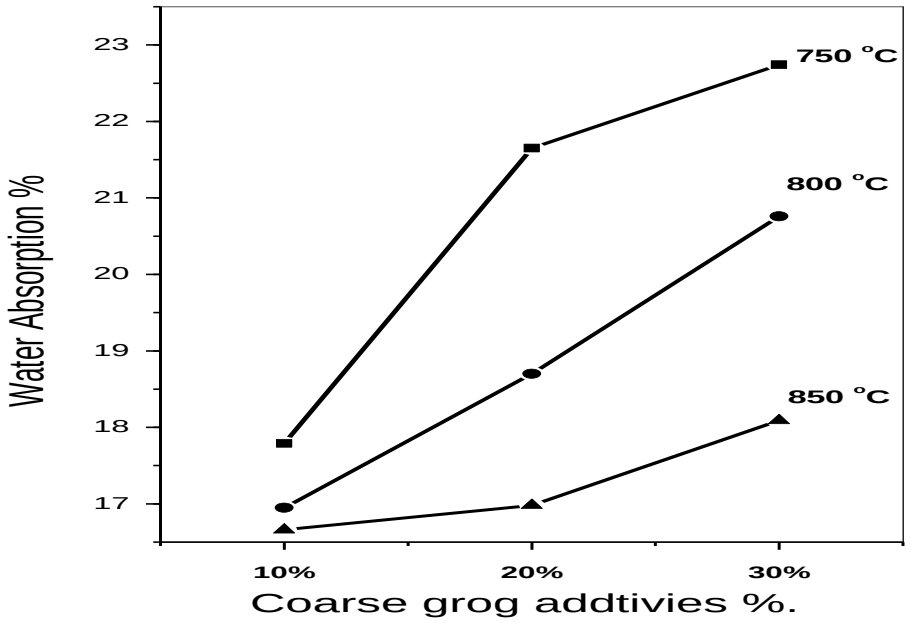

Fig (45): The relation between the water absorption and corase grog additives percent.

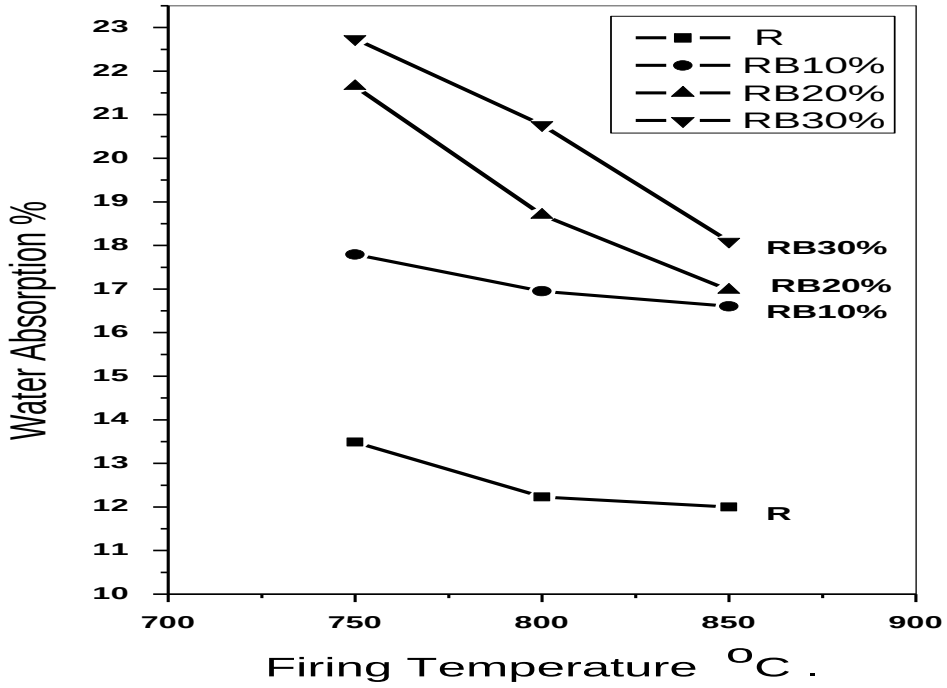

Fig (46): The relation between the water absorption and coarse grog additives with firing tempratures.

Table (16) summarizes the results of the water absorption of fired samples with various percentages of studied additives (sand, grog, saw dust) with firing temperatures.

Table (16): The water absorption of fired samples.

Symbol	Water Absorption %			
	750 ^{o}C	800 ^{o}C	850 ^{o}C	Additives type
R	13.49	12.23	12.00	Blank
RS40%	16.8	16.47	16.26	Sand addition
RA10%	15.45	13.032	12.43	Fine grog addition
RA20%	16.16	15.56	13.31	
RA30%	17.84747	17.33181	15.30073	
RB10%	17.795	16.954	16.661	Coarse grog addition
RB20%	21.657	18.708	16.985	
RB30%	22.7402	20.765	18.0986	
RC5%	18.2	17.85	17.4	Sawdust addition
RC10%	20.37	18.76	18.56	

The water absorption increases with increase of the additive% (sand, grog, sawdust) in the batch. That can be attributed to that the additives facilitate passage of water. Water absorption decreases with increase of firing temperatures because the extent of vetrification enhances which close some of open pores leading to discontinuous pore system.

3.4.4. The apparent porosity.

The values of the apparent porosity of the fired samples against percentage of additives, sand, sawdust and grog, as function of the firing temperatures were illustrated extensively.

3.4.4.1. Effect of Sand.

Table (17) and Figure (47) show the change of the apparent porosity of the fired samples with sand content and with firing temperatures respectively.

As show from Table (17), the apparent porosity of the fired samples increases remarkably with increase of sand content in the batch. From Fig (47) it is clear that, the apparent porosity of the fired samples decreases with increase of firing temperature for all batches.

Table (17): The apparent porosity of (R, RS40%) samples.

Symbol	Apparent Porosity, %			
	750 ^{o}C	800 ^{o}C	850 ^{o}C	Additives type
R	25.63	24.29	23.85	Blank
RS40%	30.60	29.9	29.8	Sand addition

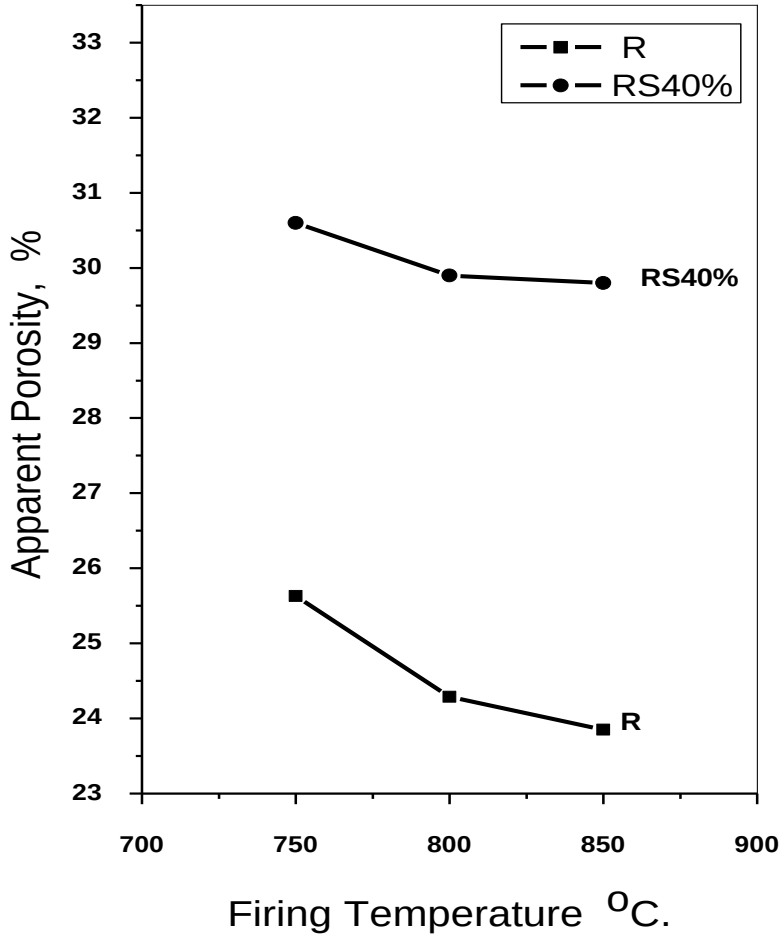

Fig (47): The relation between the apparent porosity and sand additive with firing temperatures .

3.4.4.2. Effect of Saw dust.

Figures (48, 49) show the change of the apparent porosity of the fired samples with saw dust (as replacement to sand) content and with firing temperature respectively.

As shown from Figure (48) the apparent porosity of the fired samples increases with increase of saw dust for all firing temperature. From Figure (49) it is clear that, the apparent porosity of the fired samples decreases with increase of firing temperatures for all batches

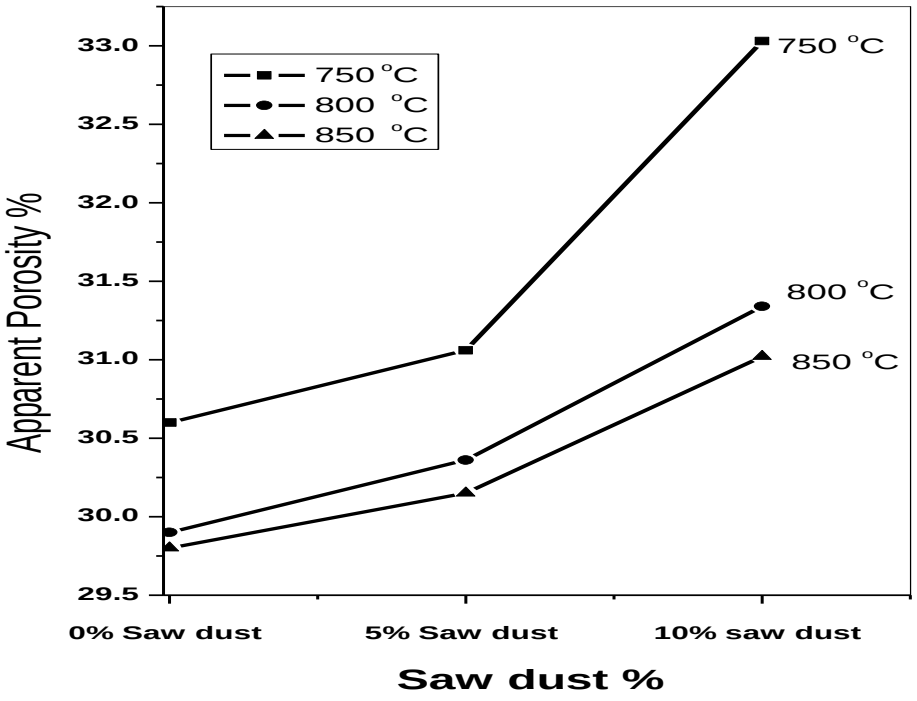

Fig (48): The relation between the apparent porosity and sand, sawdust additives percent .

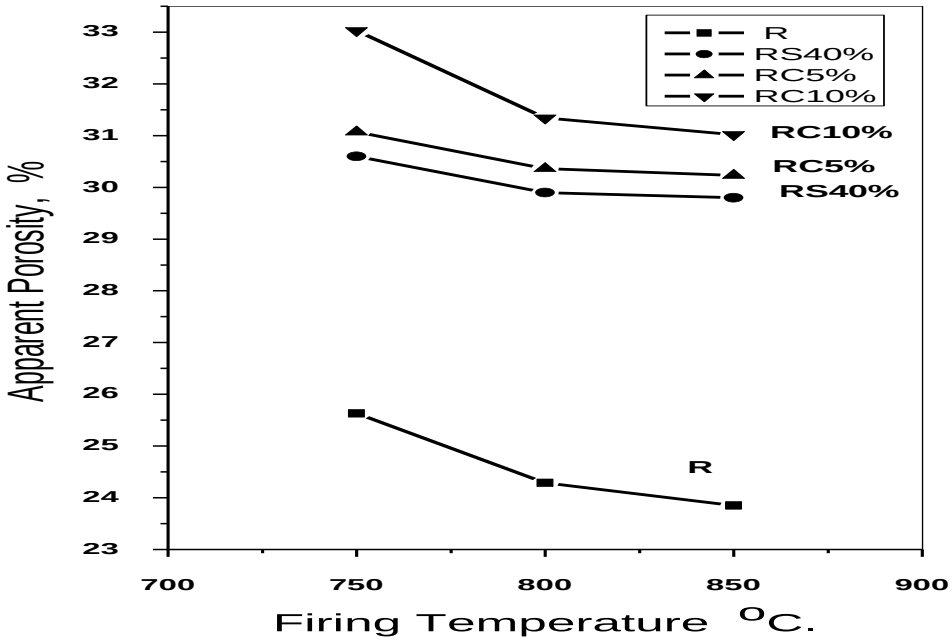

Fig (49): The relation between the apparent porosity and sand,sawdust additives with firing temperatures .

3.4.4.3. Effect of fine and coarse waste fired bricks (Grog).

Figures (50, 51) show the apparent porosity of the fired samples with fine grog content and with firing temperatures respectively.

As shown from Figure (50) the apparent porosity of the fired samples increases remarkably with increase of fine grog content in the batches. From Figure (51) it is clear that, the apparent porosity of the fired samples decreases with increase of firing temperatures for all batches.

Figures (52, 53) show the apparent porosity of the fired samples with coarse grog content and with firing temperatures respectively.

As shown from Figure (52) the apparent porosity of the fired samples increases remarkably with increase of coarse grog content in the batches. From Figure (53) it is clear that, the apparent porosity of the fired samples decreases with increase of firing temperatures for all batches. From Figures (50-53) it is clear that, the coarse grog addition has more considerable effect on the apparent porosity of the fired samples than fine grog.

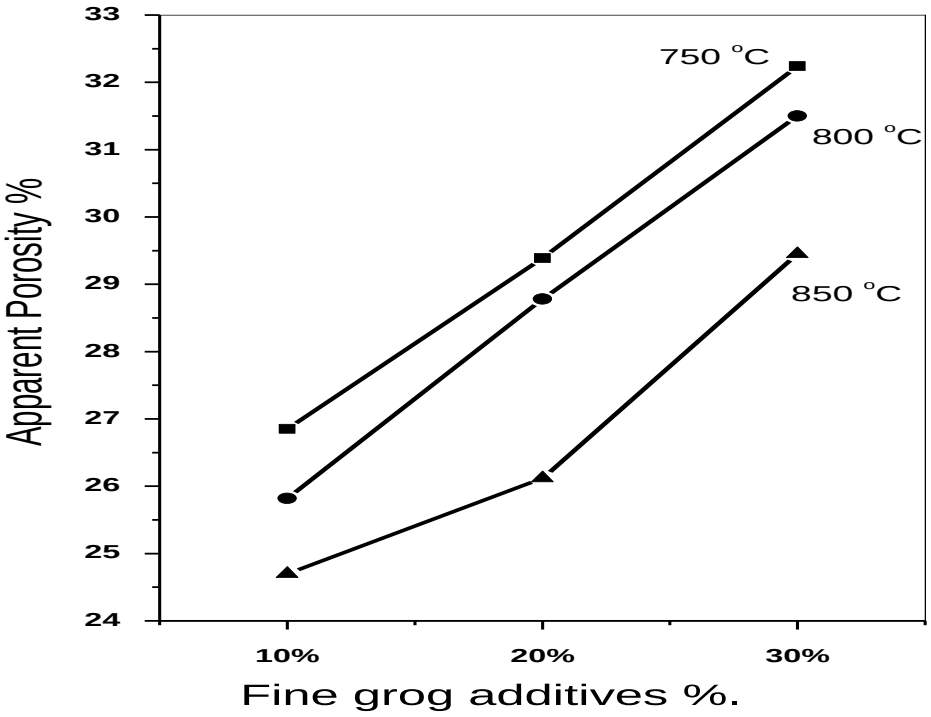

Fig (50): The relation between the apparent porosity and fine grog additives percent .

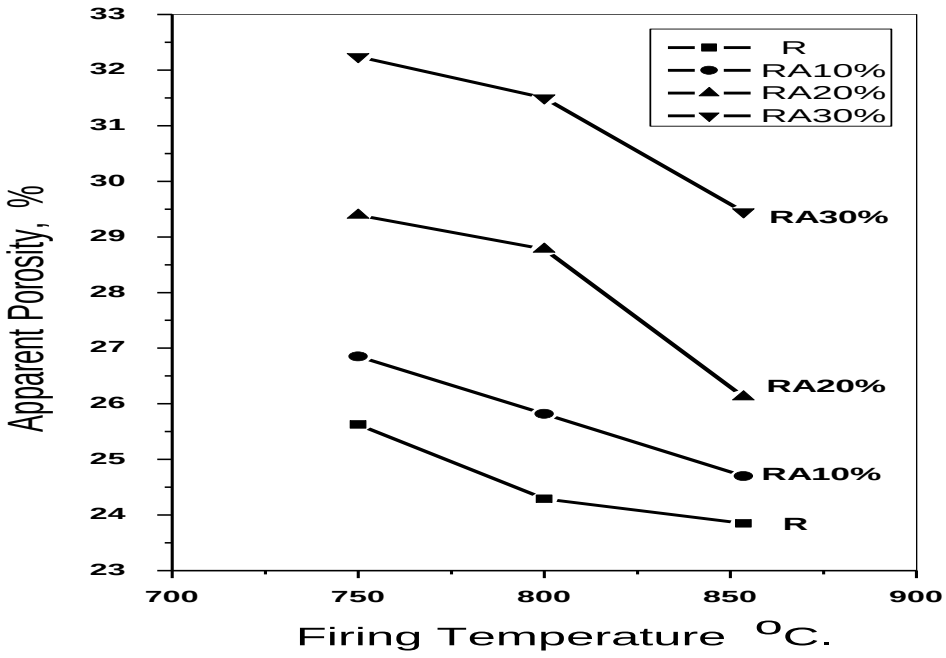

Fig (51): The relation between the apparent porosity and fine grog additives with firing temperatures .

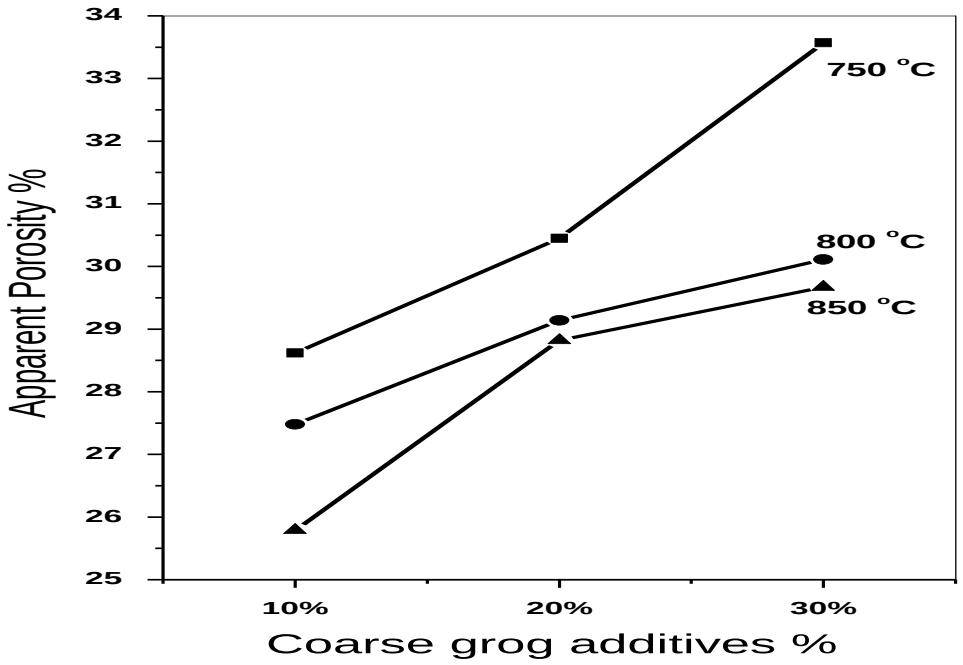

Fig (52): The relation between the apparent porosity and coarse grog additives percent .

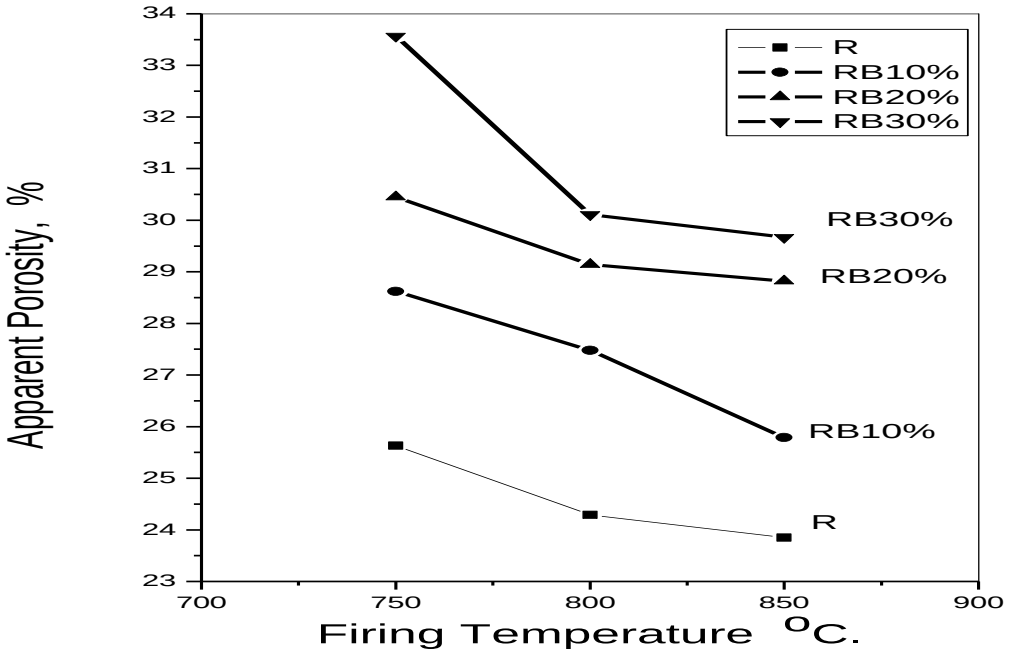

Fig (53): The relation between the apparent porosity and coarse grog additives with firing temperatures .

Table (18) summarizes the results of the apparent porosity of fired samples with various percentages of studied additives (sand, grog, saw dust) and with firing temperatures.

Table (18): The apparent porosity of fired samples.

Symbol	Apparent Porosity, %			
	750 ^{o}C	800 ^{o}C	850 ^{o}C	Additives type
R	25.63	24.29	23.85	Blank
RS40%	30.60	29.9	29.8	Sand addition
RA10%	26.85	25.82	24.70	Fine grog addition
RA20%	29.39	28.78	26.12	
RA30%	32.24	31.50	29.45	
RB10%	٢٨,٦٢	٢٧,٤٨	٢٥,٧٩	Coarse grog addition
RB20%	٣٠,٤٥	٢٩,١٤	٢٨,٨٢	
RB30%	٣٣,٥٧	٣٠,١١	٢٩,٦٧	
RC5%	31.06	30.36	30.15	Sawdust addition
RC10%	33.030	31.34	31.02	

Apparent porosity of the brick samples increases with increase of additive content in the clay batches. The additive opens up the microstructure pore systems of the brick samples. The apparent porosity decreases with increasing the firing temperature because the extent of vitrification increases which closes some of open pores of the body leading to a discontinuity of the open pores. Apparent porosity decreases in the sequence (sawdust > coarse grog > fine grog > sand).

3.4.5. The bulk density

The values of the bulk density of the fired samples against percentage of additives, sand, sawdust and grog as function of the firing temperatures were illustrated extensively.

3.4.5.1. Effect of Sand.

Table (19) and Figure (54) show the change of the bulk density of the fired samples with sand content and with firing temperatures respectively.

As show from Table (19), the bulk density of the fired samples decreases remarkably with increase of sand content in the batch. From Fig (54) it is clear that, the bulk density of the fired samples increases with increase of firing temperature for all batches.

Table (19): The bulk density of (R, RS40%) samples.

Symbol	Bulk Density g/cm^3			
	750 ^{o}C	800 ^{o}C	850 ^{o}C	Additives type
R	1.87	1.92	1.95	Blank
RS40%	1.82	1.81	1.83	Sand addition

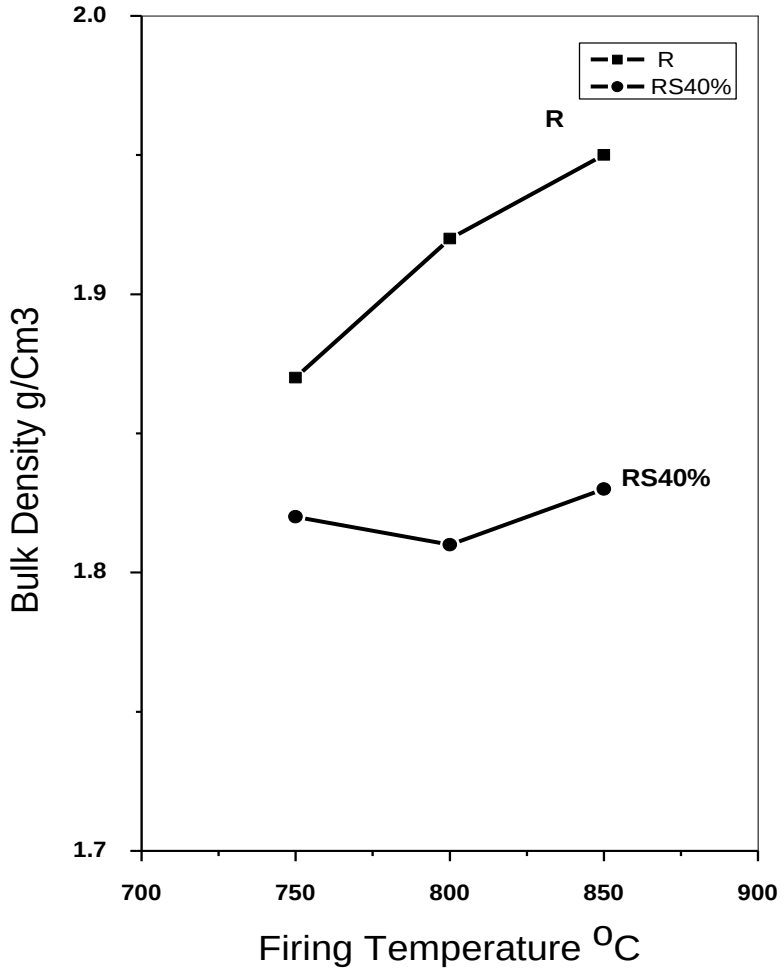

Fig (54)**:** The relation between the bulk density and sand additives with firing tempertaures .

3.4.5.2. Effect of Saw dust.

Figures (55, 56) show the change of the bulk density of the fired samples with saw dust content (as replacement to sand) and with firing temperature respectively.

As shown from Figure (55) the bulk density of the fired samples decreases with increase of saw dust for all firing temperature. From Figure (56) it is clear that, the bulk density of the fired samples increases with increase of firing temperatures for all batches

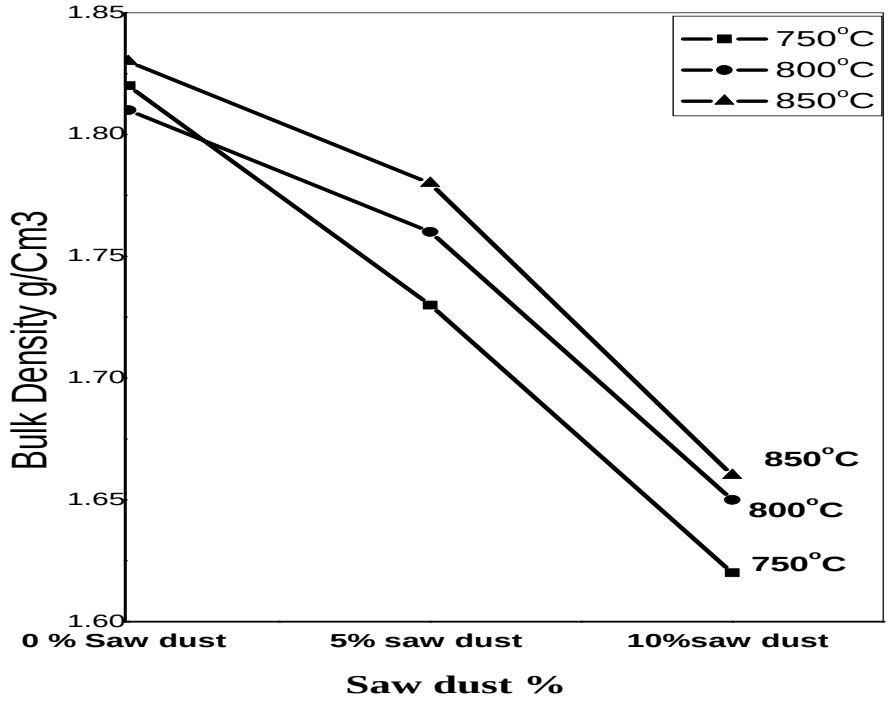

Fig (55): The relation between the bulk density and sawdust additives percent .

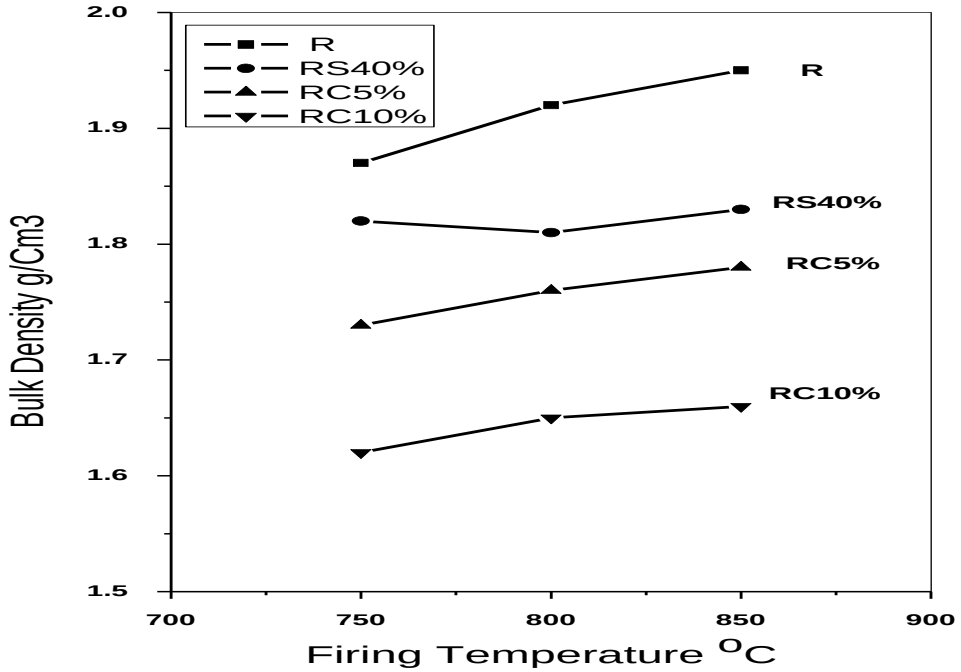

Fig (56) : The relation between the bulk density and sand, sawdust additives with firing temperatures .

3.4.5.3. Effect of fine and coarse waste fired bricks (Grog).

Figures (57, 58) show the bulk density of the fired samples with fine grog content and with firing temperatures respectively.

As shown from Figure (57) the bulk density of the fired samples decreases remarkably with increase of fine grog content in the batches. From Figure (58) it is clear that, the bulk density of the fired samples increases with increase of firing temperatures for all batches.

Figures (59, 60) show the bulk density of the fired samples with coarse grog content and with firing temperatures respectively.

As shown from Figure (59) the bulk density of the fired samples decreases remarkably with increase of coarse grog content in the batches. From Figure (60) it is clear that, the bulk density of the fired samples increases with increase of firing temperatures for all batches. From Figures (57-60) it is clear that, the coarse grog addition has more considerable effect on the bulk density of the fired samples than fine grog.

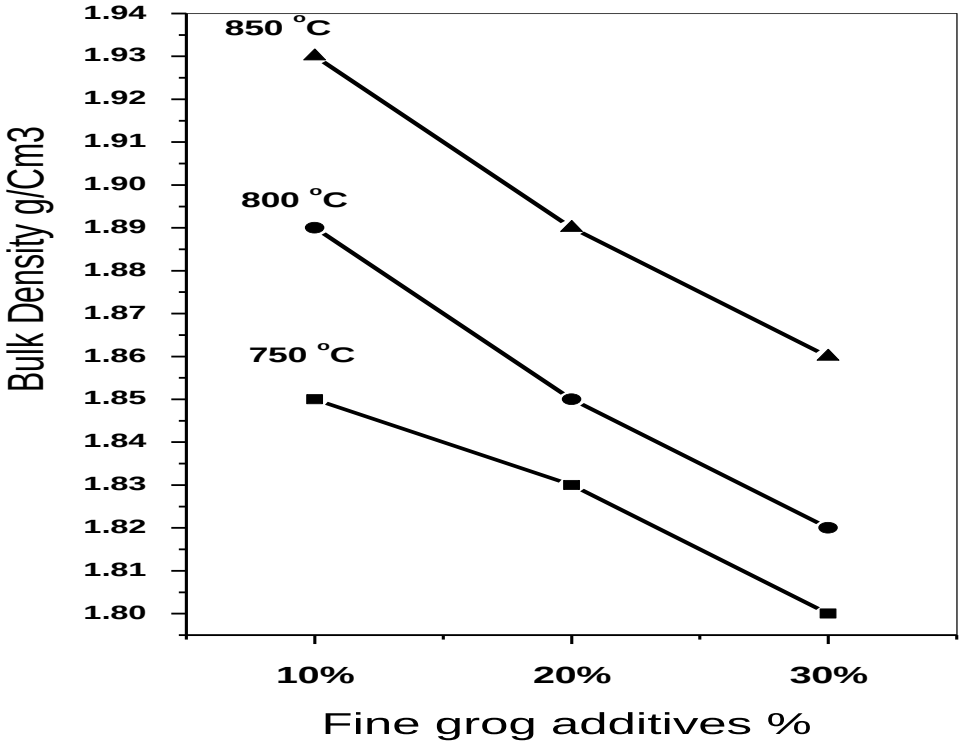

Fig (57): The relation between the bulk density and fine grog additives percent .

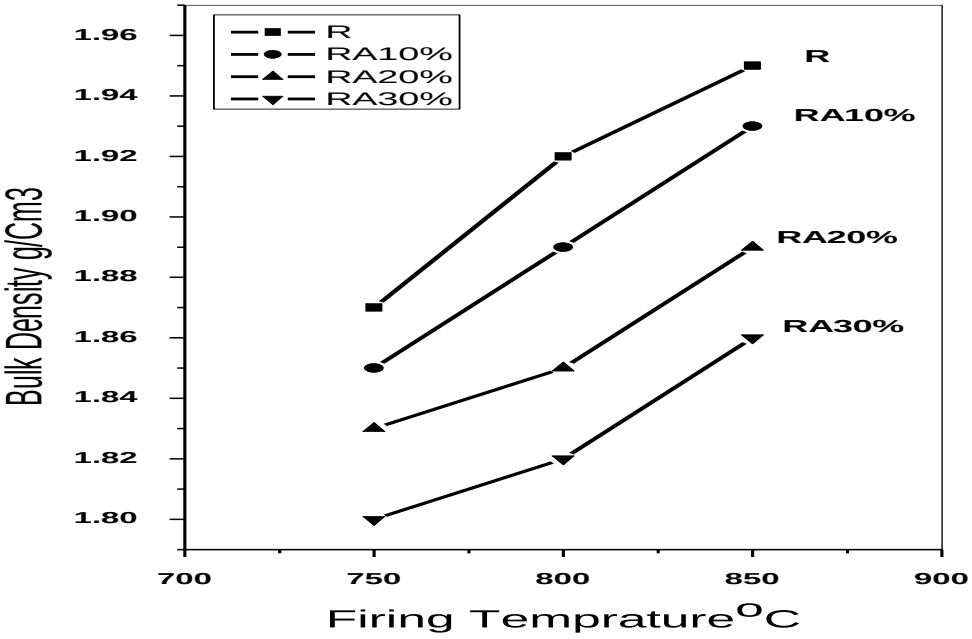

Fig (58): The relation between the bulk density and fine grog additives with firing tempratures .

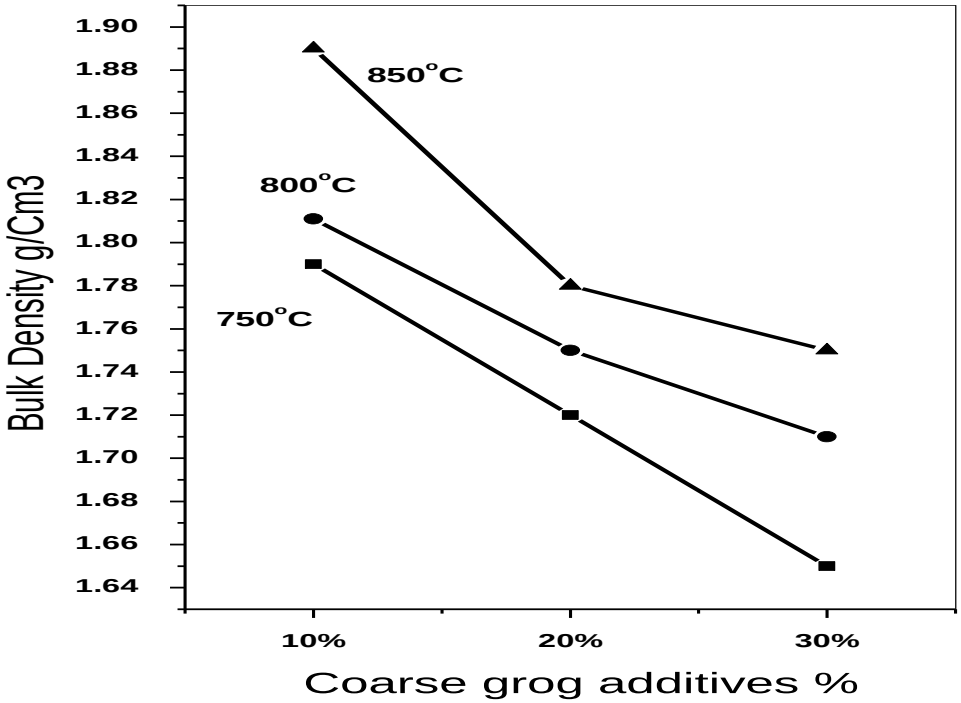

Fig (59): The relation between the bulk density and coarse grog additives percent.

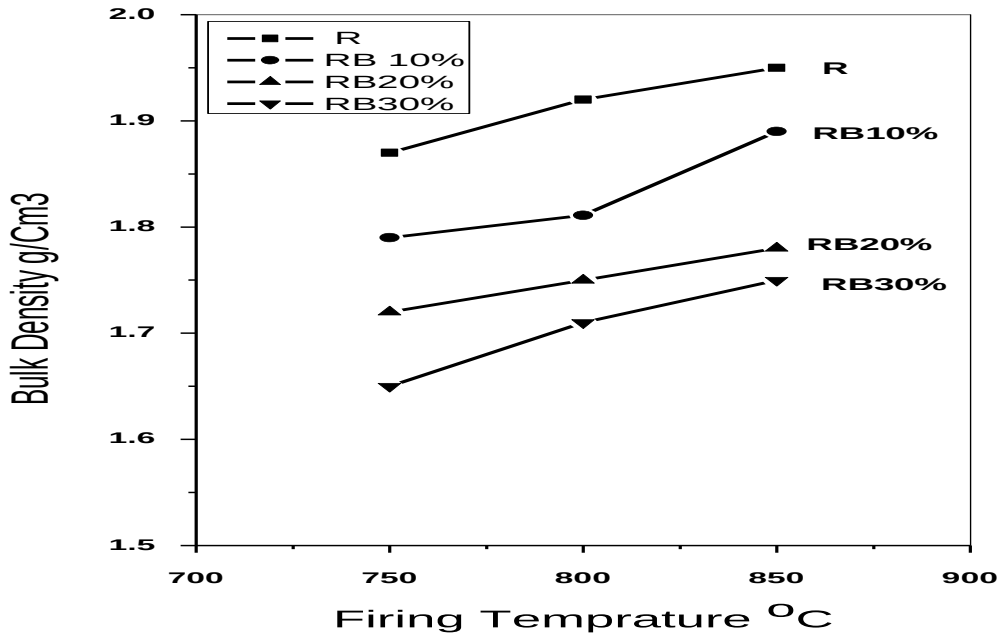

Fig (60): The relation between the bulk density and coarse grog additives with firing temperatures.

Table (20) summarizes the results of the bulk density of fired samples with various percentages of studied additives (sand, grog, saw dust) and with firing temperatures.

Table (20): The bulk density of fired samples.

Symbol	Bulk Density g/cm^3			
	750 ^{o}C	800 ^{o}C	850 ^{o}C	Additives type
R	1.87	1.92	1.95	Blank
RS40%	1.82	1.81	1.83	Sand addition
RA10%	1.85	1.89	1.93	Fine grog addition
RA20%	1.83	1.85	1.89	
RA30%	1.80	1.82	1.86	
RB10%	1.79	1.811	1.89	Coarse grog addition
RB20%	1.72	1.75	1.78	
RB30%	1.65	1.71	1.75	
RC5%	1.73	1.76	1.78	Sawdust addition
RC10%	1.62	1.65	1.66	

As clear from table (20) the bulk density decreases with increasing sand, grog, sawdust content. The variation in bulk density is nearly opposite to the water absorption and apparent porosity of clay brick samples

The bulk density increases with firing temperature because the extent of vitrification enhances and densification increases so the bulk density increases with firing temperature. Higher temperature,

aluminosilicate reacts with fluxing oxides giving some glass phase. Therefore the bulk density increases due to closing some of the open pores with glass phase formed at higher temperature .

Sawdust additives is the most effective additives in reducing the bulk density then follows the coarse grog, then fine grog (sawdust < coarse grog <fine grog < sand 40%).

3.4.6. The crushing strength.

The values of the crushing strength of the fired samples against percentage of additives, sand, sawdust and grog as function of the firing temperatures were illustrated extensively.

3.4.6.1. Effect of Sand.

Table (21) and Figure (61) show the change of the crushing strength of the fired samples with sand content and with firing temperatures respectively.

As show from Table (21), the crushing strength of the fired samples decreases remarkably with increase of sand content in the batch. From Fig (61) it is clear that, the crushing strength of the fired samples increases with increase of firing temperature for all batches.

Table (21): The crushing strength of (R, RS40%) samples.

Symbol	Crushing strength in Mpa			
	750 ^{o}C	800 ^{o}C	850 ^{o}C	Additives type
R	8.69	11.13	12.43	Blank
RS 40%	7.91	9.97	10.22	Sand addition

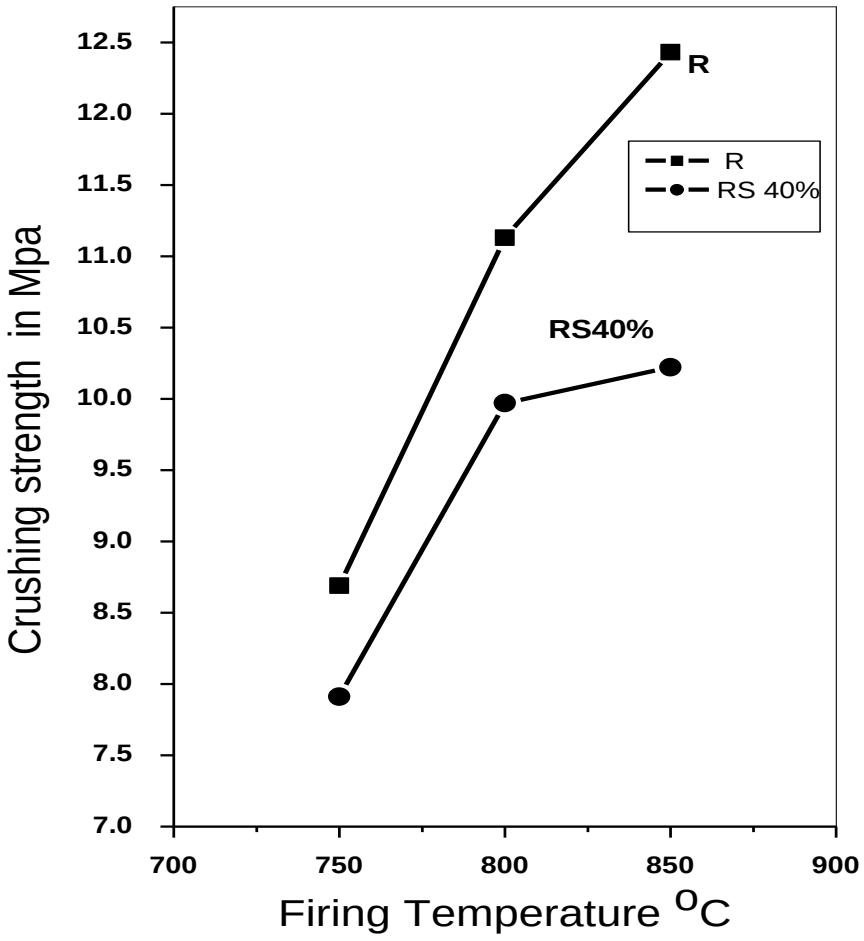

Fig (61): The relation between the crushing strength and sand additives with firing temperatures .

3.4.6.2. Effect of Saw dust.

Figures (62, 63) show the change of the crushing strength of the fired samples with saw dust content (as replacement to sand) and with firing temperature respectively.

As shown from Figure (62) the crushing strength of the fired samples decreases with increase of saw dustfor all firing temperature. From Figure (63) it is clear that, the crushing strength of the fired samples increases with increase of firing temperatures for all batches.

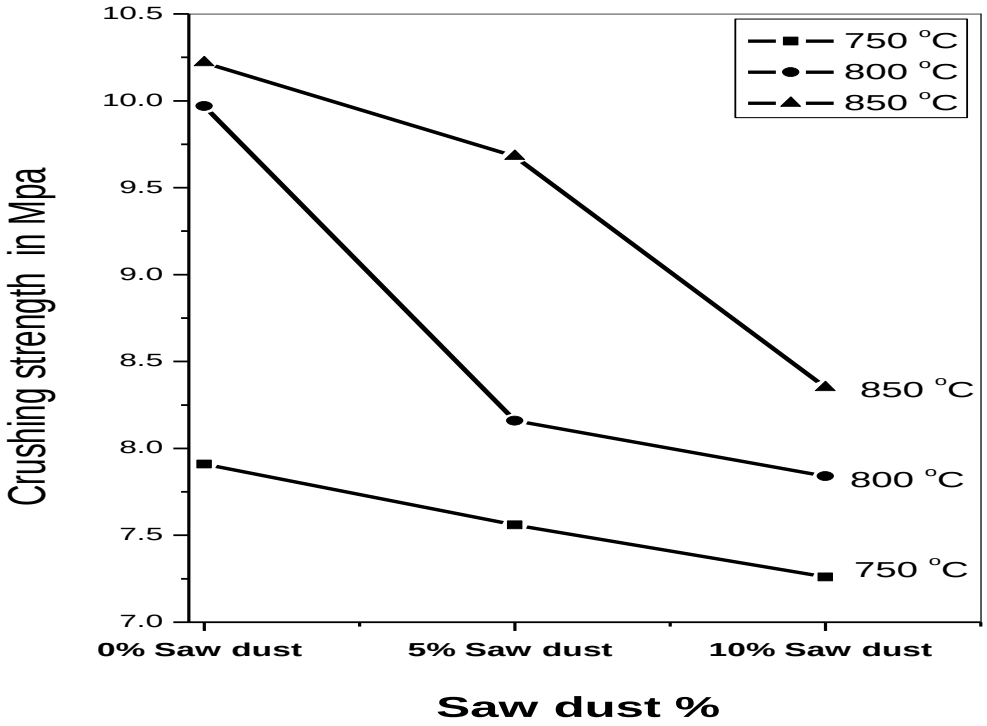

Fig (62): The relation between the crushing strength and sawdust additives percent

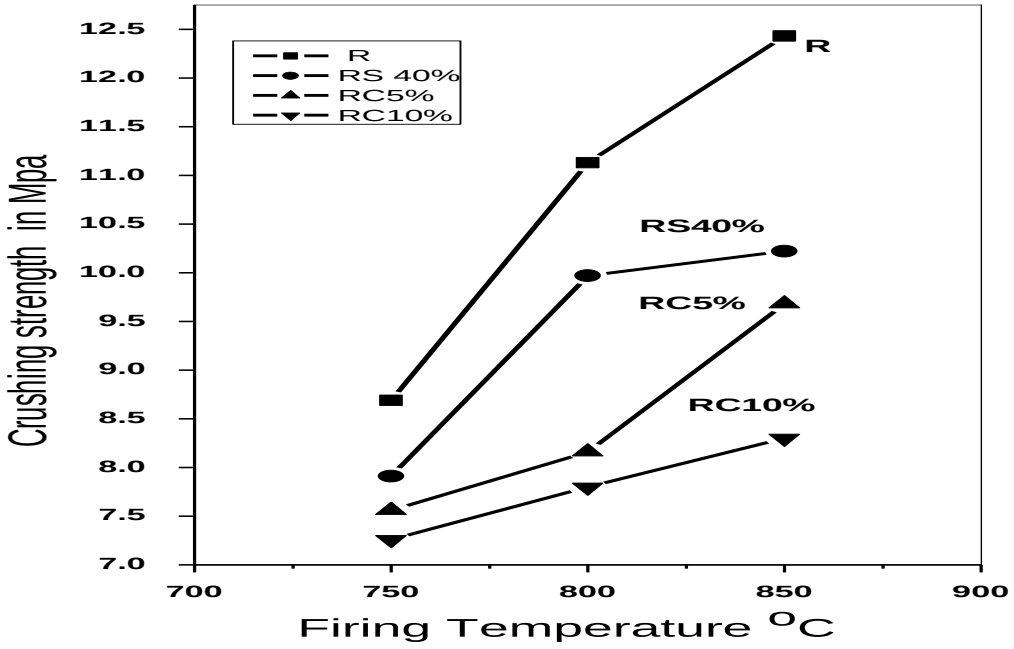

Fig (63): The relation between the crushing strength and sawdust additives with firing tempratures .

3.4.6.3. Effect of fine and coarse waste fired bricks (Grog).

Figures (64, 65) show the crushing strength of the fired samples with fine grog content and with firing temperatures respectively.

As shown from Figure (64) the crushing strength of the fired samples decreases remarkably with increase of fine grog content in the batches. From Figure (65) it is clear that, the crushing strength of the fired samples increases with increase of firing temperatures for all batches.

Figures (66, 67) show the crushing strength of the fired samples with coarse grog content and with firing temperatures respectively.

As shown from Figure (66) the crushing strength of the fired samples decreases remarkably with increase of coarse grog content in the batches. From Figure (67) it is clear that, the crushing strength of the fired samples increases with increase of firing temperatures for all batches. From Figures (64-67) it is clear that, the coarse grog addition has more considerable effect on the crushing strength of the fired samples than fine grog.

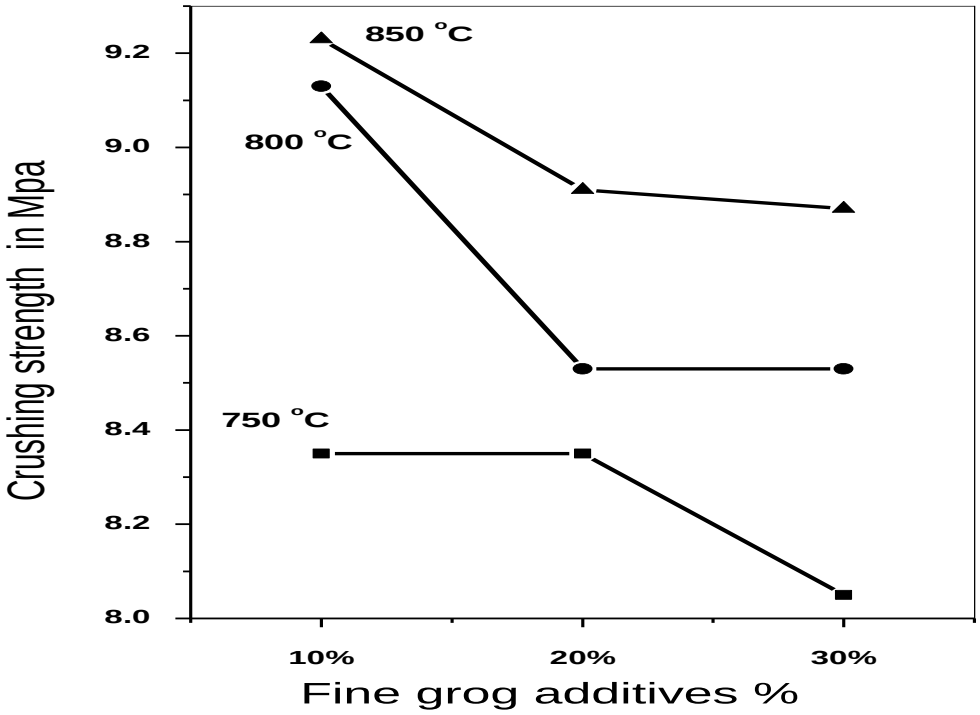

Fig (64): The relation between the crushing strength and fine grog additives percent

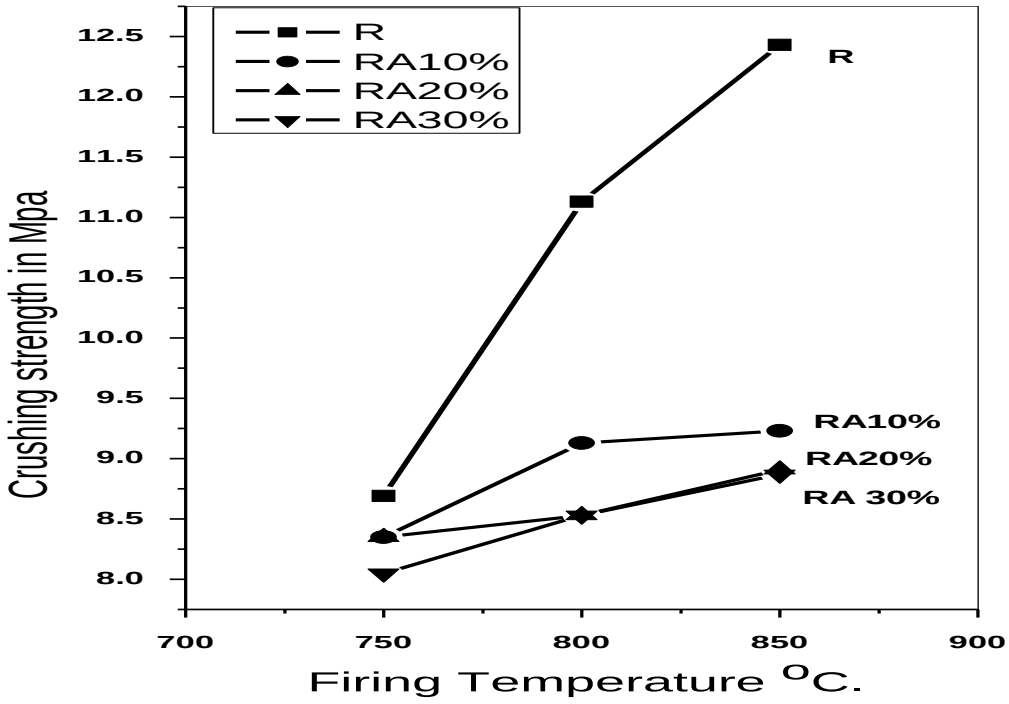

Fig (65): The relation between the crushing strength and fine grog additives with firing tempratures .

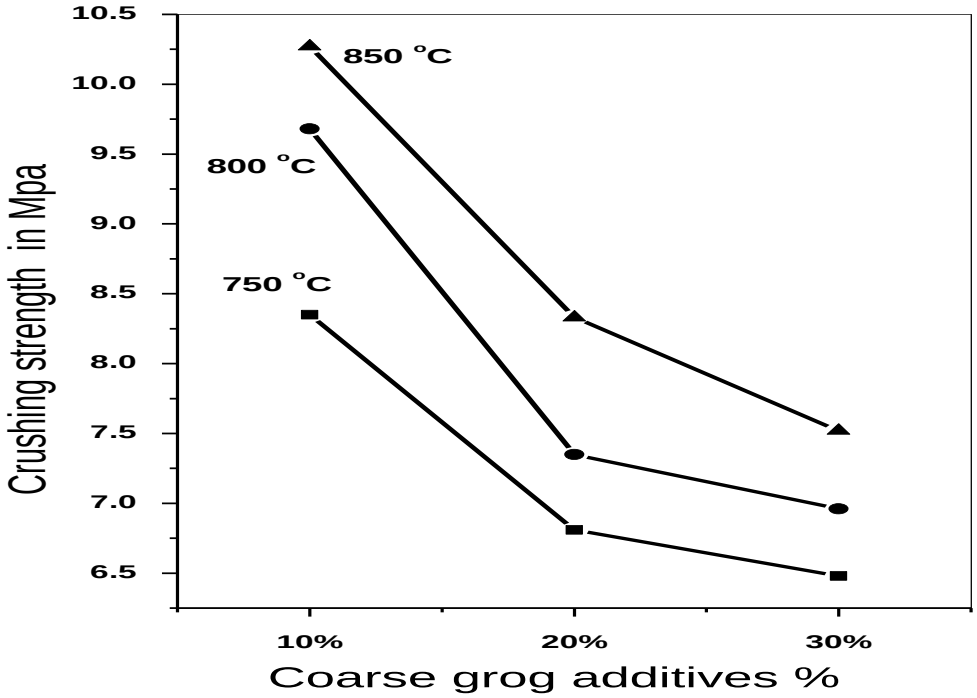

Fig (66): The relation between the crushing strength and coarse grog additives percent.

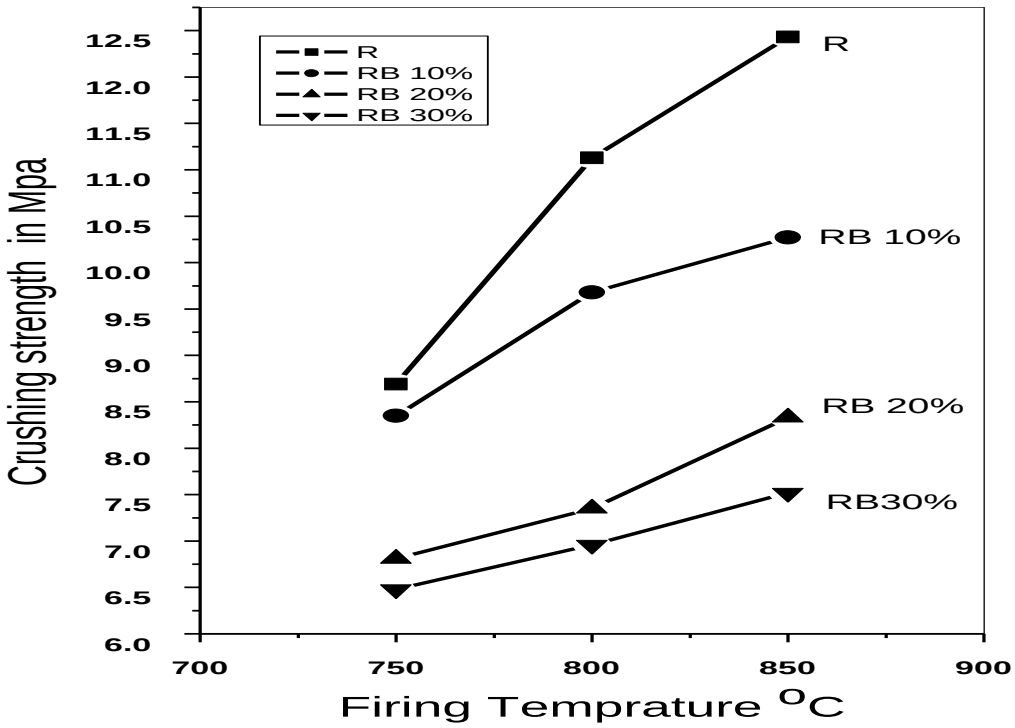

Fig (67): The relation between the crushing strength and coarse grog additives with firing temperatures.

Table (22) summarized the results of the crushing strength of fired samples with various percentages of studied additives (sand, grog, saw dust) with firing temperatures.

Table (22): The crushing strength of fired samples .

Symbol	Crushing strength in Mpa			
	750 ^{o}C	800 ^{o}C	850 ^{o}C	Additives type
R	8.69	11.13	12.43	Blank
RS 40%	7.91	9.97	10.22	Sand addition
RA10%	8.35	9.13	9.23	Fine grog addition
RA20%	8.35	8.53	8.91	
RA30%	8.05	8.533	8.87	
RB10%	8.35	9.68	10.27	Coarse grog addition
RB20%	6.81	7.35	8.33	
RB30%	6.48	6.96	7.52	
RC 5%	7.56	8.16	9.68	Sawdust addition
RC 10%	7.26	7.84	8.35	

The crushing strength decreases with increasing sand, grog, sawdust content because the apparent porosity increases .In fact that can represent criteria for the available percent of additives.

The crushing strength increases with firing temperature because the extent of vitrification enhances densification. At higher temperature aluminosilicate reacts with fluxing oxides giving some glass phase ,

therefore the crushing strength increases due to closing some of open pores with glass phase formed at higher temperature .

Coarse grog additives is the most effective additives in reducing the crushing strength then follows the fine grog (coarse grog <fine grog < sawdust < sand 40%).